Optimization of a microfluidic assay for the detection of free prostate cancer specific antigen

Miguel Ângelo Freitas Ribeiro Gaspar Reis

Thesis to obtain the Master of Science Degree in

Biotechnology

Supervisor(s): Prof João Pedro Estrela Rodrigues Conde
Dr. Narayanan Srinivasan Madaboosi

Examination Committee

Chairperson: Prof. Luís Joaquim Pina da Fonseca
Supervisor: Prof. João Pedro Estrela Rodrigues Conde
Members of the Committee: Dr. Pedro Carlos de Barros Fernandes

November 2014

Abstract

The elevated number of false positives in prostate cancer (PCa) tests have demonstrated the need to design a multiplex assay capable of crossing information from various PCa biomarkers in order to provide a more reliable diagnosis. A miniaturized microfluidic ELISA was optimized in order to detect clinically relevant concentrations (1-4 ng mL^{-1}) of free prostate specific antigen (f-PSA). A microfluidic device comprised of microchannels was microfabricated with polydimethyl siloxane (PDMS) through soft lithography and sealed to a glass slide. The ELISA parameters such as molecules concentration, incubation time, flow rate and blocking methodology were optimized. The detection of concentrations in the ng mL^{-1} range were reached using fluorescence, chemiluminesce and colorimetry methods. Microscope imaging parameters for all three detection methods were optimized. Colorimetry detection was also measured by amorphous silicon (a-Si:H) *p-i-n* photodiodes. Calibration curves based on the detection of f-PSA spiked solutions was constructed. Detection limits were calculated for all the three detection methodologies.

Keywords

ELISA, Microfluidics, Prostate cancer, PSA, Biomarkers, Photodiodes

Resumo

O elevado número de falsos positivos em testes de cancro da próstata (PCa) têm demonstrado a necessidade de criar um ensaio multiplex capaz de cruzar informação de vários biomarcadores do cancro da próstata, ao ponto de fornecer um diagnóstico mais fidedígno. Um ELISA miniaturizado foi otimizado a fim de detectar concentrações clinicamente relevantes (1-4 ng mL^{-1}) de *free prostate specific antigen* (f-PSA). Um dispositivo microfluidico composto de microcanais foi microfabricado com dimetil polisiloxano (PDMS), por meio de litografia e selado a uma lâmina de vidro. Os parâmetros do ELISA, como a concentração de moléculas, o tempo de incubação, taxa de fluxo e metodologia de bloqueio foram optimizados. Foram detetadas concentrações na ordem do ng mL^{-1} com os métodos de fluorescência, quimioluminescência e colorimetria. Parâmetros de imagem do microscópio para todos os três métodos de detecção foram otimizados. Deteção da colorimetria também foi efectuada em fotodíodos de silício amorfo hidrogenado (a-Si: H) *p-i-n*. As curvas de calibração foram construidas com base na deteção de soluções com f-PSA. Os limites de detecção foram calculados para todos as três metodologias de deteção.

Palavras-chave

ELISA, microfluídica, cancro da próstata, PSA, Biomarcadores, Fotodíodos

Acknowledgements

I would like to thank Professor João Pedro Conde for the opportunity to work in his group at INESC-MN and the direction and guidance throughout the project. To my co-supervisor, Dr. Narayanan Srinivasan with whom I shared a project and a laboratory and whom I thank for all the availability and guidance throughout my work. I also thank Dr. Virginia Chu for the support. To Ruben Soares for all discussions and company throughout the the laboratory work. Engineers Virginia Soares, Fernando Silva and José Bernardo for training and assistance during the microfabrication processes in the cleanroom. To all my colleagues with whom I shared my daily life and endless discussions. I would still like to thank Eunice Paisana for helping me with the correction of the written work.

Finally I would like to thank my parents and my brother and my sister who always believed in me and never stopped supporting me throughout my academic career.

Agradecimentos

Gostaria de agradecer ao Professor João Pedro Conde pela oportunidade de poder trabalhar no seu grupo no INESC-MN e pela orientação e acompanhamento durante todo o projecto. Ao meu co-orientador, Dr. Narayanan Srinivasan com quem partilhei um projecto e um laboratorio e a quem agradeço toda a disponibilidade e orientação durante todo o meu trabalho. Agradeço também á Dr. Virginia Chu o apoio demonstrado. Ao Ruben Soares por todas as discussões e apoio. Aos engenheiros Virgínia Soares, Fernando Silva e José Bernardo por a formação e ajuda durante os processos de microfabricação na sala limpa. A todos os meus colegas de trabalho com quem partilhei o meu dia a dia e infindáveis discussões. Gostaria ainda de agradecer á Eunice Paisana pela ajuda na correção do trabalho escrito.

Por último gostaria de agradecer aos meus pais e irmãos que sempre acreditaram em mim e nunca deixaram de me apoiar durante todo o meu percurso académico.

Contents

List of Figures

List of Tables

Abbreviations

a-Si:H	**H**ydrogenated **a**morphous **Si**licon
BPH	**B**ening **P**rostatic **H**yperplasia
BSA	**B**ovine **S**erum **A**lbumin
CaSR	**Ca**lcium **S**ensing **R**eceptor
EPCA	**E**arly **P**rostate **C**ancer **A**ntigen
ELISA	**E**nzyme **L**inked **I**mmuno**S**orbant **A**ssay
FITC	**F**luorescein **I**so**T**hio**C**yanate
fPSA	**f**ree **P**rostate **S**pecific **A**ntigen
emt-PSA	**e**qui**m**olar **t**otal **P**rostate **S**pecific **A**ntigen
GPI	**G**lycosyl**P**hosphatidyl**I**nositol
HRP	**H**orse**r**adish **P**eroxidase
LoC	**L**ab **o**n **C**hip
LoB	**L**imit **o**f **B**lank
LoD	**L**imit **o**f **D**etection
LoQ	**L**imit **o**f **Q**uatitation
MEMS	**M**icro**E**lectro**M**echanical **S**ystems
PD	**P**hoto**D**iode
PoC	**P**oint **o**f **C**are
PDMS	**P**oly**D**i**M**ethyl**S**iloxane
PMMA	**P**oly **M**ethyl **M**eth**A**crylate
PAP	**P**rostate **A**cid **P**hosphatase
PCa	**P**rostate **C**ancer
PSA	**P**rostate **S**pecific **A**ntigen

PSA-ACT	**P**rostate **S**pecific **A**ntigen - **A**nti**C**hymo**T**rypsin
PSMA	**P**rostate **S**pecific **M**embrane **A**ntigen
PSCA	**P**rostate **S**tem **C**ell **A**ntigen
SSDNA	**S**almon **S**perm **D**eoxyribo**N**ucleic **A**cid
SAM	**S**elf **A**ssembly **M**onolayer
SD	**S**tandard **D**eviation
TMB	3,3',5,5'- **T**etra**m**ethyl**b**enzidine

Motivation

Microfluidics is a multidisciplinary field which has gained perceivable notability in the recent years due to the advantages it provides over standard methodologies for the execution of laboratorial tasks in a microscale.

Prostate cancer is the second most prevalent form of cancer globally. On top of this, the screening test is controversial due to the high number of false positives. There is a need for the development of a multiplex test involving several PCa biomarkers in order to validate the screenings results, reducing the false positives ratio and improving early detection of this cancer form.

With this in mind, this work attempted at an optimization of an assay for the detection of prostate cancer biomarkers in a microfluidic device, trying to simplify and reduce costs on the top bench task involved by miniaturizing the process.

The present work is divided into four chapters. In the introduction, a theoretical approaches is presented along with the state-of-the art. Materials and methods present all the methodologies and materials used during the experimental procedures. The results obtained from the experimental work are presented and analyzed. Discussion of the results is in the last chapter along with the conclusions of the work and future prospects.

Chapter 1

Introduction

1.1 Clinical Diagnosis

1.1.1 Point of Care (PoC) analysis

Point of care analysis is presented now-a-days as the most valuable method for patient testing due to the advantages it conveys over the standard laboratory testing. PoC testing has already gained a considerable percentage of the *in vitro* diagnostics market however this is due to the large diabetes monitoring chains in it. Outside the diabetes market, the use of PoC devices for diagnostic purposes is a bit more controversial partially due to sensitivity and reliability issues [3, 4].

The main concept behind PoC is to have the patient tested on the spot returning the results instantly which allows for immediate course of action to be taken by the diagnostic entity. This brings up many doubts about the quality and reliability of the results presented by such test due to user handling variations [3, 5]. Alongside with the difficulty of integration of all laboratory procedures into a single device, PoC devices development still presents many other challenges. Fluid handling tasks such as fluid delivery, mixing, and separation of analyte from the sample mix are simple tasks to handle in a laboratory which need to be integrated into such device. The aim is to develop a fully integrated and

automated miniaturized system able to perform samples analysis with high sensitivity and accuracy on a single portable platform [6, 7].

In the last few years microfluidic platforms have demonstrated to be efficient in integrating different modules for sample processing, leading towards a fully automated analysis system. Microfluidics also show other useful characteristics for developing PoC devices such as reduced production costs and high sensitivity as well as accuracy [3, 6]. Digital microfluidics, multiphase flow systems and multielectrode arrays are a few other platforms that may provide the tools needed for PoC diagnostics [6, 8].

Digital Microfluidics (DMF), for instance, is an interesting technology since it eliminates the need for external pneumatic controls and valves in order to control reagent and sample flows. DMF concept is to manipulate sample volumes the size of a droplet. These droplets are driven over a micropatterned plate which uses an electrowetting mechanism based on the surface energy changes due to applied potential. This allows for different steps to be programmed and executed orderly, making the manipulation sequence similar to the bench-top procedure using micro litre volumes, higher automation and considerably less time [9, 10].

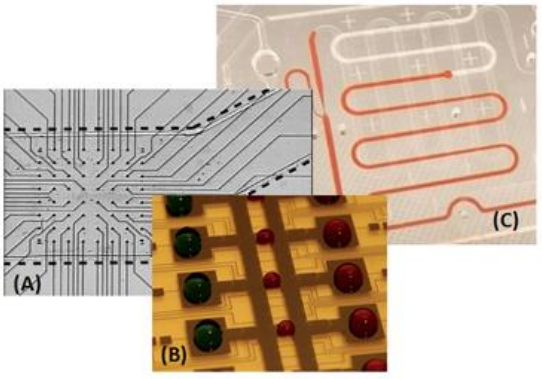

FIGURE 1.1: (A) Microelectrode array device (adapted from F); (B) Digital microfluidic device (Adapted from G); (C) microfluidic platform (adapted from [1, 2])

1.1.2 Lab-on-chip (LoC)

In light of all these new technology, comes forward a new concept named Lab-on-chip. In this concept is embedded the idea of developing a miniaturized laboratory on a

chip which can perform complex top-bench tasks, reducing reagents waste and the time of the analysis itself. Such devices are millimetres to few square centimetres in size. LoC's belong to a subset category of MEMS (Microelectromechanical systems) and are often based on microfluidic technology in such a way the physicals principals behind such device are withdrawn from the microfluidics field. All this is manageable on a microscale due to the difference in behaviour of fluids at this scale. The manipulation of amazingly small volumes (nano to pico litres) also allows for a more accurate control of the concentrations and interactions between liquids[11].

Lab on a chip technology can be applied to a wide variety of clinical analysis. The most common is in the measurement of blood sugar levels by diabetic patients. This technology may also be used for the detection of biomarkers for liver failure, kidney damage and CVD's (cardiovascular diseases). Not only for biomarkers but also for the detection of virus, LoC's technology may bring forward great progress. LoC is particularly useful since it provides a platform for miniaturization of standard ELISA analysis used for biomarkers and viral clinical analyses [4, 12–14]. One interesting use of LoC devices is the miniaturization of PCR assays. The application of these devices for quantitative PCR and Real-time PCR is another aspect demonstrating the versatility of the LoC concept [15]. All these different procedures may be adapted to the LoC concept allowing for complete techniques such as PCR, flowcitometry, microarrays, aqueous two-phase systems to be integrated into a single device [15].

This requires for different detection methods to be integrated into such devices. This includes labelled antibodies with HRP-enzyme (chemiluminescence), fluorophores (fluorescence), which light emission can be detected through the use of a microscope or in a much more integrated and simplistic manner, through the use of photodiodes [16]. Another possibility is to have a Streaming current system to perform measurements of a solution through functionalization of the assay's surface.

Overall, the LoC concept provides in-numerous advantages in comparison with most of the current methods used. Such advantages include: reduction of reagent and sample volumes; faster analysis (faster reactions inside the device, mostly due to the size and scaling effect); easier control of various environmental parameters such as concentration,

temperature and chemical reactions time; portability; automation; higher throughputs; lower fabrication costs.

However some disadvantages also arise, these being: the experimental conditions may not always scale down in a positive manner leading to further complications; signal-to-noise ratios; lack of accuracy in microfabrication in comparison with bigger scale engineering [17, 18].

1.2 Prostate cancer (PCa)

Prostate cancer is now-a-days one of the leading causes of cancer related deaths in men, particularly in the western countries, being the most prevalent form of sickness in Europe. WHO statistics register about 200 000 new cases of prostate cancer every year.

The prostate tumour grows penetrating peripheral tissues (perineural invasion) such as lymphatic channels and nodes. The lymphatic nodes are the most likely tissue to host the first metastases. [19, 20] After the metastases spread into the blood stream, one of the first targets are the bone structure, forming osteocleorotic metastases [21].

1.2.1 PCa biomarkers

A significant variety of biomarkers are known for PCa, although each one with different characteristics and different reliabilities, presenting different pieces of information about PCa. From proteins to mRNA and also metabolites concentrations such as calcium may be measured for obtaining information on tumour development.

Prostate stem cell antigen (PSCA), for instance, is a GPI-anchored cell surface protein found in blood that depicts with a reasonable degree of accuracy the progression of PCa (PSCA-1). High expression of this protein is observed in about 90% of prostate cancer patients. As for PSCA-2 it is known to have a Jekyll and Hyde molecule behavior and is known to be presented in high values in cases of bladder and pancreatic cancer [22–24].

Prostate specific membrane antigen (PSMA) is another PCa biomarker found in tissue, serum and cells. PSMA is a zinc metalloenzyme residing in membranes facing the extracellular space. It is thought to be one of the most upregulated proteins in prostate tissue, going up has far as 12-fold when compared to noncancerous patients. However it has been reported increased expression also in other tissues such as the brain, liver and kidneys, therefore requiring calibration strategies when taking into account PSMA concentration in a clinical analysis [25].

Prostatic acid phosphatase (PAP) is another serum enzyme which upregulation carries indication of prostate cancer although it is not a very reliable analysis. A variation in Calcium concentration is also known to be an indicator of a disturbance in the homeostasis. A direct correlation between the increase in calcium concentration and the development of a prostate tumor may be established. These changes in the concentration are due to the change in the expression of a calcium sensing receptor (CaSR) which affects the calcium intake [26].

Many other biomarkers possess relevance in the diagnosis and prognosis of PCa. Some of these are EPCA (Early prostate cancer antigen), GOLPH2 (Golgi phosphoprotein 2) and even sarcosine [27]. Nevertheless, a consensus on values for diagnostic purposes does not exist yet among the scientific community on these biomarkers. There is one though which has awakened some interested in the last few years. This is prostate-specific antigen.

1.2.2 Prostate Specific Antigen

One of the most prominent PCa biomarkers is PSA (Prostate-specific antigen), used particularly for early diagnosis and also for monitoring the progression of the tumour, also known as kallikrein-3 (KLK3) is a glycoprotein enzyme from the kallikrein-related peptidase family, secreted by the epithelial cells of the prostate gland. PSA may allow the detection of PCa as much as 5 years before symptoms start. Although this molecule is intended to dissolve cervical mucus facilitating the sperm entrance in the uterus, small quantities of it roam in the circulatory serum. Since this protein has a proteolitic

function, the biggest percentage in the serum is a complexed form of PSA bound to another protein, most commonly α1-antichymotrypsin (PSA-ACT) or α2-macroglobulin (PSA-A2M). This is because of the proteolitic activity of this protein requires a silencing protein to be coupled to PSA in order to inhibit its activity.

Nevertheless, a non complexed form of PSA exists in the blood current in a small percentage being designated free PSA (fPSA). The ratio between the two different forms helps distinguishing between a possible PCa or BPH (Benign Prostatic Hyperplasia) diagnosis. Also the ratio may change in a significant way just so that information concerning the evolution of a tumour may be extrapolated. In healthy men PSA is present in very small amounts in the serum whereas in the case of prostate disorders the values are more elevates.

Keeping in mind that every man has different basal PSA values, some calibration of these values is required in order for a relevant reading of values. This is where the ratio between the fPSA and PSA-ACT comes in. The total amount of PSA in the serum (both fPSA and PSA-ACT) is designated by tPSA (total PSA) [19, 20, 28].

Thinking in a multiplex approache for the analysis of various molecules in the same assay, another prostate molecule comes into play. Kallikrein-2 is also a prostate specific serine protease similar to PSA. The similarities go as far as having similar epitopes which generate cross-reactivity with PSA antibodies. This molecule has shown to be highly expressed in poorly differentiated cancer cells. Also it has shown to be related to PSA activity since it is involved in the process of converting the percursor form of PSA to active PSA. This can become a relevant molecule for the differentiation between PCa and BPH [29].

1.2.3 PSA antibodies

The use of PSA antibodies in ELISA testing is the standard in clinical laboratories tests, therefore it becomes important to define the quality and relevance of the antibodies chosen. For fPSA and PSA-ACT, anti-fPSA and anti-PSA-ACT antibodies respectively are used for measuring these molecules concentrations. In terms of measuring the overall

amount of both forms of PSA a standard anti-tPSA antibody has proven to be inefficient by presenting different affinities for the two different PSA forms. It would happen that anti-tPSA antibody would have more affinity to the complexed form since it is present is a higher concentration. This led to the development of equimolar total PSA (emt-PSA). This antibody maintains the same affinity for fPSA and PSA-ACT independently of the concentration of each one avoiding an over or underestimation. This way PSA ratio can now be measured more efficiently [30]. Using the emt-PSA antibody we have a capture system for two different molecules (the fPSA and PSA-ACT) which affinities are not affected by the targets' concentration therefore allowing for a correct measurement of both in a single assay.

1.3 ELISA

The enzyme-linked immunosorbent assay (ELISA) is a technique which makes use of antibodies to detect the presence of target molecules in different types of samples. This technique uses the principals of immunology to capture the molecules of interest. Signal detection in ELISA is usually done through some form of quantification of light emission from the reaction mixture. Even though the assay has been adapted several times to become more reliable and profitable the general methodology has remained unaltered since its implementation in the early seventies. ELISA is nowadays the standard diagnostic tool in terms of metabolite quantification in liquid samples. This also makes ELISA a good quality-control check for further tools developed by the medical research industry.

1.3.1 ELISA methodologies

Two different strategies are used when planning an ELISA test. An ELISA signal comes from a source of light coupled to the detector antibody. This detector antibody may be a primary antibody or secondary antibody depending on the chains of events of the ELISA strategy. In a direct ELISA the detector antibody (the antibody coupled with a light emitting enzyme) is linked directly to the antigen (target molecule).This usually

only allows for one antibody to link to the antigen which may translate into a weak signal depending on the concentration of the antigen.

There is however another strategy called indirect ELISA in which the enzyme-coupled antibody is not specific for the antigen of interest. These antibodies are called secondary antibodies and their specificity is to mouse antibodies. In this strategy the primary antibody (specific to the antigen) is not coupled to any enzyme and simply binds to the antigen. After this first incubation, step the secondary antibody is added to the mixture and binds to the primary antibody. This allows for the binding of more than one secondary antibody to the primary antibody, therefore increasing the signal. The indirect assay carries some advantages over the direct approach, these being the larger number of binding sites for the coupled antibody (which amplifies the signal), and the availability of an enzyme-coupled antibody for assays with different antigens, since the secondary antibody binds to whichever mouse cloned antibody that may be used.

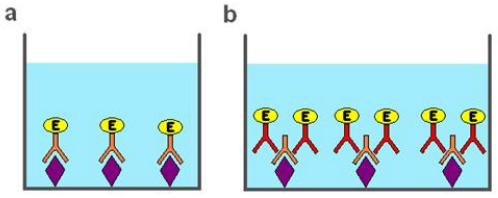

FIGURE 1.2: (a) Direct ELISA, with antigen coated on surface (purple) and enzyme-coupled (yellow) antibody (orange) bound on top; (b) Indirect ELISA, with antigen coated on surface (purple), specific non-conjugated antibody (orange) bound to the antigen and enzyme-coupled (yellow) antibody (red) bound to the specific antibody.

1.3.2 ELISA assays

Sandwich ELISA is one the most common ways to use ELISA. In this methodology, a surface is coated with a capture antibody for the antigen of interest. Then, the remaining free surface is block usually with bovine serum albumin (BSA) or salmon sperm DNA (SSDNA) and only after this step, the testing sample is run on this functionalized surface. Finally, the detection antibody (an enzyme-coupled antibody specific for a different epitope of the antibody) is added, binding to the antigen already trapped in the primary antibody. A washing step is always required after each incubation step.

The signal measured in the detection step is directly proportional to the concentration of the antigen in the tested sample.

A different way to do an ELISA is by performing a competitive assay. The strategy for measuring concentration is different in both. Unlike the sandwich assays, in a competitive assay, the signal read in the detection step is inversely proportional to the concentration of the antigen. In this assay the surface is coated with a solution of the antigen followed by a blocking step. After this, a previous mixture of a known concentration of enzyme-coupled antibody and the testing sampled is ran in the surface functionalized with the antigen, and the remaining free antibody in the mixed solution will bind to this surface bound antigen, whilst the antibodies which bound to the free antigen will be washed away. Therefore the bigger the antigen concentration in the sample, the fewer antibody molecules will be left free to bind to the surface bound antigen, depicting an inverse correlation.

1.3.3 Detection

For ELISA, light emitting enzymes used are coupled to antibodies in order to detect this light for quantification. This includes fluorescence, chemiluminescence and colorimetric assays, which require the use of appropriate enzyme labels and the corresponding substrate for the detection system. Horseradish peroxidase (HRP) is one of the most commonly used enzyme and uses luminol as substrate for the production of a light emitting product (figure 3). Other substrates may be used with HRP, such as TMB (3, 3', 5, 5'-tetramethylbenzidine) and also other enzymes such as alkaline phosphatase (AP) can be used as a detection system instead of HRP. Recently the use of quantum dots (QD's) conjugated antibodies, instead of enzyme-coupled antibodies in a standard ELISA protocol. However this variation in the detection system is just a different method applied over a systematic protocol, ending up in similar results. Quantum dots are nanocrystals capable of emitting light in different wavelength depending on its size. These are new approaches to the detection systems integrated in ELISA. [31, 32]

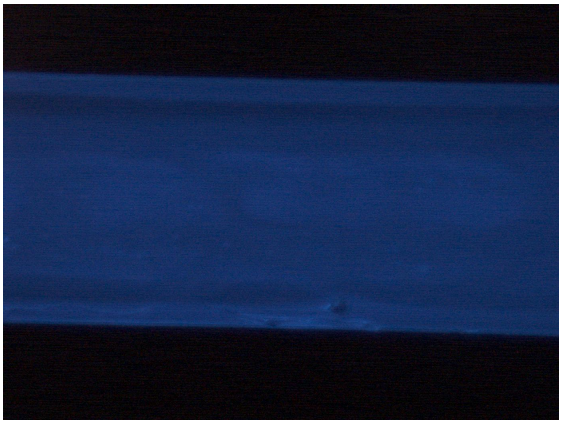

FIGURE 1.3: Microscopy photograph taken of a microfluidic channel patterned with a HRP labelled antibody. The photo was taken while running luminol though the channel at a 5 µl min^{-1} flow rate.

1.3.4 Disadvantages

Every detection system has its own strengths and weaknesses. HRP for instance is less expensive than AP, although it is also incompatible with sodium azide, a common preservative present in antibodies commercial buffer, used to prevent microbial contamination. Furthermore the presence of metals in solution is also known to affect peroxidases activity. AP has its own issues as well. Much like HRP, alkaline phosphatase is also inactivated by some conditions and metabolites. Chelating agents, acidic pH and inorganic phosphates are some of the factors which affect AP functioning [31].

As it is clear, drawbacks are present in different steps of any ELISA protocol and these drawbacks have been the driving force for the optimization of this technique, coming up with new approaches to overcome these disadvantages. One of the most concerning disadvantages of the ELISA is the amount of wasted reagent per run, and the considerable amount of time necessary in comparison with some more recent methods. More recently, new approaches have emerged, to define a whole concept of the ELISA, and optimize this technique in order to make it more gainful. Microfluidics is the new approach which is redefining the ELISA assay making it more inexpensive and less time consuming.

1.4 Microfluidics

Microfluidics is a multidisciplinary field of engineering science which integrates biology, nanotechnology, chemistry and biotechnology into one field to develop a working miniaturized platform. Microfluidics brings forward the concept of miniaturization and integration, optimized in a way to make the best of scale reduction advantages. Improvement in the behaviour, control precision and manipulation of small volumes are perks of this approach making a bold statement in the sample analysis industry. Some of these advantages go hand-in-hand with the methodologies defined for LoC devices and it is therefore the base for the development of such devices. Other advantages of this system are small sample and reagent consumption, reduced size of the overall apparatus, low energy consumption and the difference in the physical behaviour of solution at a sub-millimetre scale.

1.4.1 Microfluidic advantages

The fact that a microfluidic device handles samples in miniaturized scale brings forth differences in the behaviour of fluids, but also specific advantages which the microscale superimposes on the macroscale devices, besides the benefits already mentioned in the LoC section. High throughput screening is one of the benefits of using Microfluidics platforms to perform chemical or biological reactions. This is because Microfluidics provides the integration of all sample manipulation steps into one small area of device, allowing for the parallel duplication of the same steps, delivering a greater number of results in less time and with less reagents consumption. The easy manipulation of the device design and Microfabrication steps are also great advantages. The need to experiment with different designs in science research may sometimes delay the progress of said research.

Microfluidics devices are mostly fabricated through the use of molds, which carry the design of the device and stamp this design onto polymers as polydimethylsiloxane (PDMS).

This way, the manipulation of the design of new microfluidic devices is almost solely dependent on the time consumed on the fabrication of a new mold because this same mold maybe be used several times to stamp silicon based polymers.

Another improvement provided by microfluidics is the possibility to perform an assay using only passive diffusion, removing the need for automated systems which require a power source. This makes the fabrication process even more practical and less expensive. The fact that you have no actuation in a device makes it more reliable in the long term since the mechanical wear and tear are of less concern. Again, since there is no movement of physical components, it becomes easier to have reproducible results, making it again a more reliable way to perform a given task. All of these advantages aligned with the simplicity of a device with no moving parts make the mass production extremely inexpensive when compared to more complex devices.

A number of different actuation components have already been implemented into microfluidic devices. This is the field of MicroElectroMechanical Systems (MEMS). This field devises microdevices ranging from 1µm to 100µm in size. Some examples of this actuation structures are microvalves, micropumps and micromixers. These structures may be piezoelectrically, electromagnetically or even electrostatically actuated. Nevertheless the design of these structures has evolved in order not to rely on active actuators but instead use the passive diffusion driving force to actuate these structures. This is called passive actuation and allows for MEMS components to move without an external power source.

1.4.2 Physical Principals

The miniaturized system is based on the same reactional principals of the macroscale reactions however, because of the reduction in the design scale, these principals have different effects on the reagents. This is true for physical principals such as capillary diffusion, adsorption, liquid surface tension and velocity of the reaction. In the macroscale, capillary diffusion may not play an important role due to the larger volumes dealt with. However in the microscale, the capillary forces weight an enormous relevance and can

be used to manipulate liquid flow without the need for external pressure application. This importance is partially due to the liquid surface tension forces which also become more relevant in the microscale. Liquid surface tension has a similar scaling effect when miniaturized and surface forces become relevant for the manipulation of a microfluidic system. In the case of surface tension, it may hamper the miscibility of some solutions, or it may be helpful as in the case of digital microfluidics (DMF), a droplet based application of microfluidics, providing support for standalone droplets manipulation. Molecule diffusion in small volumes also becomes more relevant, since chemical and biochemical reactions are very fast and in macroscale diffusion coefficient is often limiting the assay velocity. Since microfluidics deals with smaller volumes, the diffusion coefficient limitation does not limit the reaction's velocity because molecules do not have to diffuse into such a greater volume allowing for a much faster assay.

All of these differences relate to the exponent of the dimension. Linear dimensions decrease slower than area or volume dimensions because of the smaller exponent. In the same way, negative exponent dimensions decrease even slower with a linear decrease.

1.4.3 Polydimethylsiloxane

The PDMS is a silicon-based organic polymer. It possesses many relevant qualities which justify its common use as substrate in microfluidic structures. It is optically clear, inert, non-toxic, allows for gas exchanges and non-flammable and has flexible surface chemistry, low permeability to water and low electrical conductivity. It is also widely used in caulking, lubricating oils, heat-resistant tiles and for the fabrication of contact lenses. PDMS has the chemical formula presented in (1), where n is the number of the monomer repetitions. [33]

CH3[Si(CH3)2O]nSi(CH3)3

(1.1)

PDMS can be fabricated by soft-lithography. This technique consists of replicating structures through the use of elastomeric stamps, molds and photomasks. This way it provides a fast and inexpensive method for replication and prototyping. The methodology is based on the stamping of an elastomer with a master mold and allows for the design of features down to 20 µm in size. It also allows for the PDMS stamping to be performed in a laboratory ambient eliminating the need to work inside a cleanroom [33, 34].

Other polymers are used in the microfluidic industry depending on specific characteristic required for microfabricated devices. Some examples of choice in polymers are: polyurethane, polycarbonate, polymethyl methacrylate (PMMA), polystyrene and polyethyleneterephthalate glycol (PETG) [33].

1.4.4 Control of surface chemistry

Due to the –O-Si$(CH_3)_2$ groups, PDMS possess a hydrophobic surface. This hydrophobicity is reversed when the surface is oxidized. The oxidation of the PDMS surface is one of the necessary steps in the sealing process. This oxidation can be done by UV radiation and exposes the silanol functional groups which can be used for sealing or functionalization of the PDMS structure. This oxidized effect lasts about 30 minutes when the oxidized surface is left in contact with air. Besides sealing, the oxidized silanol groups allow for the functionalization of this surface with a range of molecules such as polyethylene glycol (PEG). PEG is commonly used to functionalize the PDMS surface creating a higher order of aggregates providing an adhesion layer for other biomolecules. This methodology is embedded in the concept of self-assembly monolayers (SAM) in which molecules assemble non-covalently to a reactive solid surface [33, 34].

1.5 Detection Limits

When developing new structures or methods for quantification of a specific substance detection limits are important to be defined.

For the development of a new analytical method, validation and figuring of the detection limits and system sensitivity are required by the regulatory agencies worldwide. There are differences in the methods used for the calculation of different detection limits. These detection limits include various parameters such as the limit of blank (LoB), limit of detection (LoD), limit of quatitation (LoQ) and instrument detection limit (IDL) and method detection limit (MDL). For new techniques to be accepted by the regulatory organism such as Food and Drug Administration (FDA), European Medicines Agency (EMA) and United States Pharmacopoeia (USP) some rules need to be followed in calculating these parameters. Even when describing the same parameter, some differences are depicted between definitions of a certain limit and even calculation methodologies for each of the different agencies. Furthermore there is often a need for calibration experiments to be performed by a varied number of people, in different laboratories in different time periods. This guarantees the values from each said parameters are calculated derive from the most significant spread of data.

Three of the most commonly used detection limits were calculated for this project: LoB, LoD and LoQ. The LoB can be defined as the highest apparent signal found on replicates of a blank sample (no analyte). LoD is the lowest quantity of analyte capable of being reliably distinguished from the LoB and at which detection is feasible. LoQ is defined as the lowest concentration at which the analyte can be reliably detected and quantified [35].

Chapter 2

Materials & Methods

2.1 Materials

This chapter lists the materials used in this project as well as the source and supplier.The materials are divided by the methodologies in which they were used.

2.1.1 Microfabrication

List of materials used during the aluminium mask, mold and PDMS soft lithography microfabrication.

Table 2.1: List of materials used for the fabrication of the devices involved in the project.

Material	Source
Glass	-
Polydimethylsiloxane	Sigma-Aldrich, PT
Propylene glycol monomethyl ether acetate (PGMEA)	Sigma-Aldrich, PT
Poly(methyl methacrylate) (PMMA)	Local (Acrylic Supply Store) check name
Silicon wafer	LG Siltron inc, KR
SU-8 2015	(MicroChem Corp.???) Chimie Tech Services, FR
Labx 170	Bershire, engineering clean, UK

2.1.2 Microfluidics

In this section are listed the materials used during the performance of the experiments using the microfluidic device to perform miniaturized immunological assays.

TABLE 2.2: List of materials used during the performance of the experiments.

Material	Source
Syringe tips LS20	Instech Laboratories, Inc., USA
Polyethilene tubing BTPE-90	Instech Laboratories, Inc., USA
Tubing adaptors SC20/15	Instech Laboratories, Inc., USA
Microtube Eppendorf T (1,5 mL)	Delta Lab S.L.U., ES
Syringes 1 mL	CODAN Medical ApS, DK
Eppendorf micropipette tips	Sigma-Aldrich, PT

2.1.3 Immunotechnology

This subsection presents a list of all molecules and reagents used in the microfluidic immunoassay. Subsection 2.1.3.1 lists antibodies and antigens. Subsection 2.1.3.2 lists buffers and other molecules.

2.1.3.1 Antibodies & antigens

TABLE 2.3: List of Antibodies & antigens used and their specifics.

Molecule	Host	Specificity	Epitope	Source
f-PSA Antibody (epitope)	Mouse	hf-PSA	1	Abcam
emt-PSA Antibody (epitope)	Mouse	hPSA	3	Abcam
emt-PSA HRP Antibody (epitope)	Mouse	hPSA	3	Abcam
emt-PSA FITC Antibody (epitope)	Mouse	hPSA	3	Abcam
Mouse serum Antibodies	Mouse	-	-	Sigma
α- mouse FITC Antibody	Goat	Mouse	-	Sigma
Goat serum Antibodies	Goat	-	-	Sigma
α- Goat FITC Antibody	Mouse	Goat	-	Sigma
f-PSA Antigen	Human	-	-	Abcam

2.1.3.2 Chemicals & other molecules

List of surface blocking molecules and glass cleaning agent.

Table 2.4: List of chemicals and other molecules used in the experiments.

Chemicals & other molecules	**Host**	**Source**
Bovine Serum Albumin (BSA)	Bovine	Sigma-Aldrich, PT
Salmon Sperm DNA	Salmon	Provided by IST Lab
Casein	Bovine	Sigma-Aldrich, PT
Isopropyl alcohol (IPA)	-	Sigma-Aldrich, PT

2.1.4 Detection

Substrate used for the detection in enzymatic assays, chemiluminescent and colorimetric assays. These substrate were flown in the microchannel after the incubation of the sandwich ELISA molecules and were degraded by the HRP enzyme coupled to the detector antibody producing light (in the case of luminol) or a light absorbant product which precipitates inside the channel (as it happends to the TMB).

Table 2.5: List of substrates for the enzymatic assays.

Substrate	**Source**
SuperSignal West Femto (luminol)	Thermo Scientific, UK
3,3',5,5'-Tetramethylbenzidine (TMB)	Sigma-Aldrich, PT

2.1.5 Instruments & equipment

In this subsection are listed every equipment used from the microfabrication process to the final signal acquisition step.

2.1.6 Software

List of software used to develop and devices and control the devices from fabrication to detection. The list is presented in table 2.7 along with the developer of each software.

2.2 Methods

This chapter describes the methodologies used in the fabrication of the devices developed for the immunoassays, as well as the protocols used for the execution of the experiments,

Table 2.6: List of all the equipments used for the fabrication of devices, performance of the experiments and data acquisition.

Equipment	Source
Syringe Pump NE-300	New Era Pump Systems, Inc, USA
Leica DM LM	Leica Microsystems, DE
DFC300 FX	Leica Microsystems, DE
UV-H 254	Light technologies LTD, UK
UVO-Cleaner 144AX-220	Jelight Company inc, USA
WS-650MZ Spin Coater	Laurell Technologies Corporation, UK
Nordiko 7000 Broad Ion Beam Milling system	Nordiko Technical Services Ltd , UK
Disco DAD 321	Giorgio Technology, USA
Reax 2000 Vortex Mixer	Heidolph, ES
Eppendorf Research Plus Micropipettes	Sigma-Aldrich, PT
NanoPlotter NpC2.1	GeSim, DE
Milling Machine	Fabricated at Inesc-MN
Vaccum compartment	Belart products, USA
Labnet Tabletop Mini-Centrifuge	Sigma-Aldrich, PT
Ultrasonic Analogue SRH Bath	Thermo Fisher Scientific Inc,USA
Laminar Flow BSC - EN 165	Faster, IT
Digital Hotplate SD160	Stuart, UK
Incubator INB 200	Memmert, EU
Alpha-step 200	Tencor instruments, FR
a-Si:H Photodiodes	Fabricated at Inesc-MN
AmScope	Olympus
Highlight 3100	Olympus
Keithley 237 High Voltage Source Measure Unit	Keithley, USA

data acquisition and data analysis. Section 2.2.1 covers the microfabrication steps from the aluminium mask exposure to the sealing of the PDMS onto the glass substrate. Section 2.2.2 describes the protocols and standardized parameters for the assay's execution. Section 2.2.3 presents diagrams of the immunotechnology set up devised for the project. Section 2.2.4 describes the steps and parameters executed for each of the different detection methods. Section 2.2.5 covers the analysis of the acquired data.

2.2.1 Microfabrication

1. Microfabrication Steps

   This includes aluminium mask and negative SU-8 mold fabrication, soft-lithography and baking on the PDMS and the sealing of the stamped PDMS onto a clean glass substrate.

TABLE 2.7: List of software used for handling equipment, data acquisition and data analysis.

Software	Developer
DXF Mask Converter software	Developed at Inesc-MN
AutoCad	Autodesk, Inc
ImageJ	NIH
PaintShop Pro	Corel
Leica Acquisition Software	Leica Camera AG
Origin 8	Origin Lab
MS Excel	Microsoft Corporation
Mach2 CNC control	ArtSoft CNC software company
Streaming current software	Developed at Inesc-MN (Pedro Novo)
Photodiode Acquisition Software	Developed at Inesc-MN (Pedro Novo)

(a) Aluminium mask

A glass slide was cleaned in alconox for 10 minutes over a sonicator in a hot bath. It was then rinsed with IPA and left again on the sonicator for another 10 minutes this time with water. In the end it was rinsed with IPA and dried. The following steps are outlined in figure 2.1. A 1500 Å layer of aluminium was deposited on top of the cleaned glass (figure 2. 1 b) by a Nordiko 7000 Broad Ion Beam Milling system inside a clean room, and following this a positive photoresist was lay on top of the aluminium (figure 2.1 c). The glass slide was then put under the DWL where it was exposed with the mask design previously made on AutoCAD (figure 2.1 d) and converted by DXF Mask Converter. The glass sample was then incubated with "POSITIVE PHOTORESIST DEVELOPER" to develop the exposed photoresist (figure 2.1 e), following aluminium development and finally photoresist removal (fig. 2.1 f).

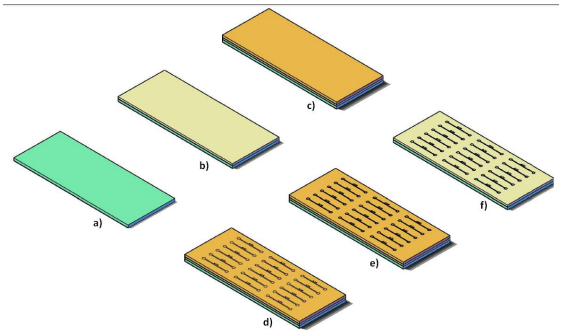

FIGURE 2.1: Schematic representation of the Aluminium mask microfabrication steps.

(b) SU-8 Mold

The negative mold used in the soft-lithography step was fabricated with negative photoresist hardened on a clean silicon wafer. The silicon wafer was cleaned by rubbing with acetone and then following the same protocol as for the previous glass slide cleaning. Negative photoresist SU-8 2015 was spilled onto the cleaned wafer and a spin coater was used to convey the photoresist with the necessary 20 µm height. The spin coater protocol used was input in the spinner as follows:

- 500 rpm, 10 seconds (100rpm/s)
- 1700 rpm, 34 seconds (300rpm/s)

The wafer with photoresist is then soft baked for 4 minutes at 95°C and is then exposed to UV light for 33 seconds through the mask previously fabricated. This step conferred the design onto the photoresist. The photoresist is then developed on PGMEA for 2 minutes, cleaned with IPA and then hard baked for 10 minutes at a temperature of 150°C.

(c) Soft-Lithography

For the PDMS device fabrication, a mixture of 1:10 of curing agent and PDMS respectively was degassed in a vacuum compartment for 30 minutes. The previously fabricated SU-8 mold was fixed inside a petri dish and after degassing the PDMS was poured inside the same petri dish and taken inside an oven at 70°C for 1h30m. The cured PDMS was cut and peeled off the petri dish bearing the original microfluidic design carved 20 µm deep. The PDMS was then punched with a syringe tip LS20 (1 mm Ø, outside diameter) in the inlets and outlets of the design in order to connect the channel to the top surface of the PDMS.

(d) Sealing

The sealing between the PDMS and glass was performed by oxidizing both halves and pressing them together. UVO oxidation can be used to alter the surface chemistry, adding silanol (SiOH) groups to the surface has shown in Figure 2.2. This was done by taking a new clean glass slide (following the

same cleaning protocol as for the mask glass slide) and the freshly peeled PDMS and inserting them both in a UVO-cleaner for 11 minutes (6 minutes of oxidation + 5 minutes for fumes exhaustion). Immediately after opening the UVO-cleaner both halves were brought together (PDMS stamped surface against glass) and left under pressure for 24 hours.

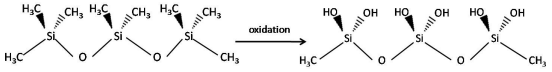

FIGURE 2.2: Oxidation effect over the chemistry of PDMS surface.

(e) Experimental Assembly

In the experimental set up, a 1 mL syringe was assembled to a polyethilene tubing BTPE-90 by a LS20 syringe tip. At the other end of the tubing a SC20/15 adaptor was attached. Through this adaptor the experimental solutions used were PUSHED in and the adaptor inserted inside the inlet hole previously punched on the PDMS device. A similar set up, only holding a small portion of tubing and an adaptor was connect to the outlet hole of the microfluidic channel to help the solution out of the microchannel. A graphic representation of the set up is shown in Figure 2.3.

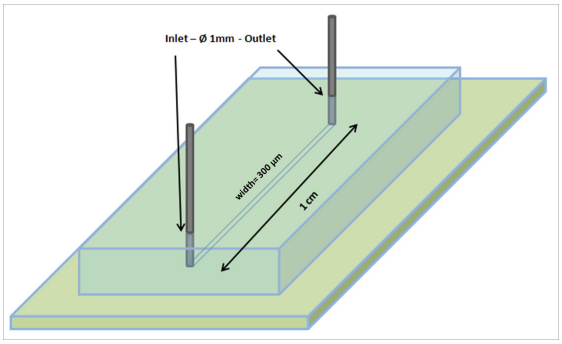

FIGURE 2.3: Representation of the assembled PDMS & glass device with adaptors inside the inlet and outlet holes.

(f) PMMA devices fabrication

PMMA devices were fabricated to serve as PDMS molding and for holding PMDS and glass structures together when sealing was not performed. Several plates (has seen in figure 2.4) had to be milled using a milling machine. The design was done in AutoCad and then converted to CNC format to be loaded

into the milling software (Mach2 CNC control).

The PMDS molding structure is presented in figure 2.4 and is composed of 3 plates. A bottom plate which holds the SU-8 microfabricated molds with the channels structure. The middle plate which defines the PDMS hight. The top plate which seals the top and possesses 1 mm Ø (diameter) holes, aligned with the inlets and outlets designed on the SU-8 mold, in which SC20/15 adaptors were inserted leaving holes on the PMDS going from the top to the bottom in order to let solutions being inserted inside the channels. Supplement 5 mm Ø holes were made on the sides in order to hold the 3 plates together with screws.

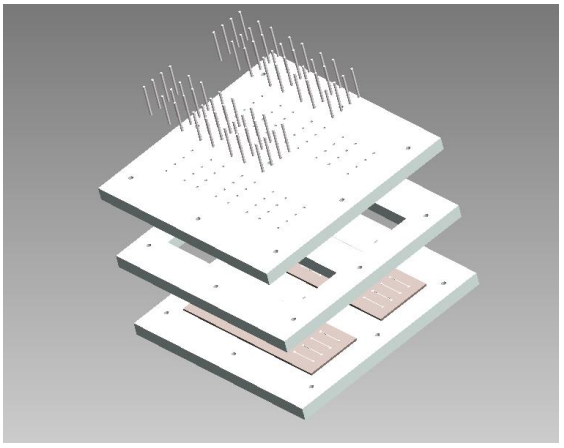

FIGURE 2.4: Schematic representation of the PMMA mold for PDMS fabrication.

The device for holding unsealed PDMS and glass together possesses only 2 plates, bottom and top, milled in a box-like shape capable of holding the PDMS fabricated in the previous device against a 0,7 mm width glass (Figure 2.5).

2.2.2 Microfluidics

1. Microfluidic Steps

   (a) Set-Up

   The syringe connected to the assembled experimental device is pumped by

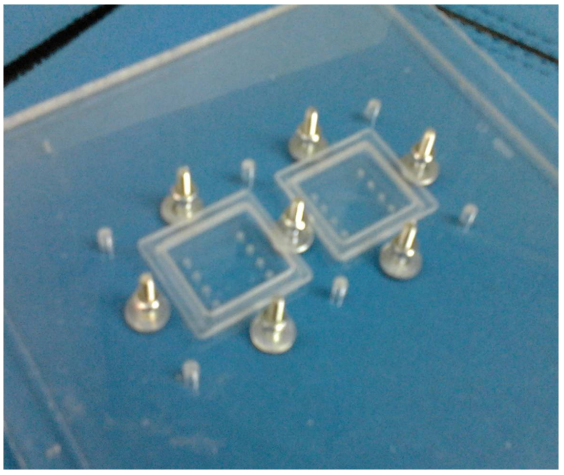

FIGURE 2.5: Photo of the fabricated device to hold unsealed PDMS and glass together.

a syringe pump at defined flow rates for a restrict amount of time, both depending on the solution used and experimental goal. Between the pumping of different solutions into the microchannel, the adaptor needs to be changed and the tip of the tubing cut off up to the point wetted by the previously solution. This prevents contamination of solutions in the eppendorfs and unwanted molecule reactions outside the microchannel.

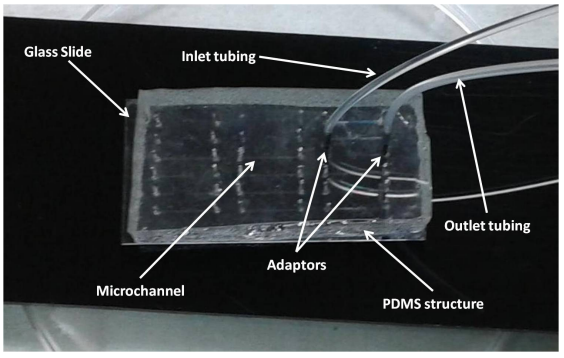

FIGURE 2.6: Photograph of the assembled PDMS & glass device with adaptors inside the inlet and outlet holes over a black PMMA plate.

(b) Experiment Standard Conditions (incubation time, flow rate and washing) Incubation for the molecules was set at 10 minutes and a flow rate of 0,5 µl min^{-1}. For BSA, the incubation time was set at 5 minutes due to the relative high concentration used (4% BSA). The washing steps were performed with

PBS 10mM (also used for molecules dilution) and a 5 µl min^{-1} flow rate was used for 1 minute.

Capture antibody (f-PSA specific antibody) was incubated under constant flow on the channel at 0.5 µl min^{-1} for 10 minutes. After every incubation step a 1 minute washing step was performed. Followed the BSA incubation step and then the analyte spiked solution of f-PSA. Finally the detector labelled antibody (FITC or HRP) was incubated and a final wash performed. In the case of HRP labelled antibody a detection solution (luminol or TMB) was incubated during imaging.

2.2.3 Immunotechnology

1. Immunotechnology

   (a) Diagram

The schematic approach used for the miniaturized ELISA is shown in figure 2.7. In this molecular set up capture antibody for free PSA is incubated and the free space is filled with BSA (smaller molecule - 66.5 kDa) in order to block the adsorption of the detector antibody to the surface. The free PSA is then incubated and binds to the capture antibody and in the final step detector antibody is incubated and binds to the free PSA bound to the capture antibody.

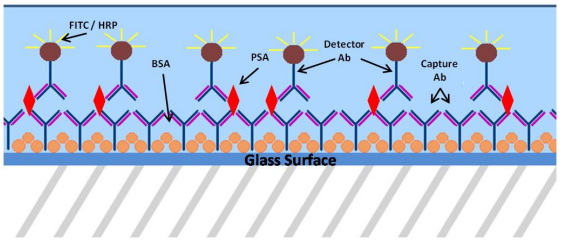

FIGURE 2.7: Schematic representation of the sandwich ELISA set up using f-PSA, f-PSA specific antibodies and BSA for blocking step. This set up is assembles inside the microfluidic channel onto a glass surface.

(b) Methodology

An miniaturized ELISA was the approach chosen to be performed in a microfluidic device for the detection of f-PSA molecules. However incubation conditions were optimized for the scaling of the experiment with the goal of reduced assay time and reducing the volume of reagents and samples necessary.

2.2.4 Detection

1. Detection methods

(a) Fluorescence

Fluorescence detection was performed using IgG labelled with FITC molecules. After incubation and adsorption of the labelled IgG the channel was exposed with a fluorescence light (100 Watts) under the microscope and imaged through a fluorophore filter with an illumination path between 450-490 nm and a observation path of 515 nm.

(b) Chemiluminescence

Chemiluminescence detection is based on an enzymatic degradation step by the HRP-enzyme (Horseradish Peroxidase) of a substrate (luminol) which emits a blue light during the enzymatic reaction. HRP-labelled IgG was incubated in the microchannel and after incubation and final washing, the whole experimental set-up was moved to the microscope side and the device was put under the microscope still attached to the syringe which now carried luminol to be run on the same microchannel in which the HRP-IgG was incubated. The microscope was then cover with a black cloak which prevented the outside light reaching the device and in total darkness the luminol was flown in the channel at 0,5 µl min^{-1} for all the duration of the imaging step.

(c) Colorimetry

As for the chemiluminescence detection, colorimetry also makes use of the HRP enzymatic activity to degrade a substrate. Only in this case the substrate does not glow. Instead it deposits on the microfluidic channel blocking

the transmittance of the microscope white light. The experimental set up was moved to the microscope side and TMB was run. Since the enzymatic reaction product deposits on the channel, time of TMB incubation become relevant. TMB was run for 2 minutes at 0,5 µl min^{-1}.

(d) Photodiodes

For the acquisition of a signal with photodiodes, one of the previous methods would be chosen and same conditions as used for the microscope would be emulated on a PCB wire-bonded to the photodiodes.

2.2.5 Image Acquisition Analysis

1. Acquisition Parameters

(a) Exposure, Gain, Gamma

Table 2.8 shows the values of exposure, gain and gamma used for each one of the detection techniques imaged under the microscope. For colorimetry however the microscope white light was set to maximum power with the condenser fully open. For both fluorescence and chemiluminescence the microscope illumination was turn off.

TABLE 2.8: Parameters used for the imaging of each detection methodology.

Detection	Exposure	Gain	Gamma
Fluorescence	1 second	1	0,6
Chemiluminescence	10 seconds	10	0,6
Colorimetry	500 µseconds	1	0,6

(b) ImageJ Analysis

The images acquired were analysed in terms of signal intensity through the use of ImageJ. In each picture equal sections were selected inside the microchannel and three other equal sections were selected outside the channel to be used as background. The signal from the background sections was subtracted to

the corresponding signal of the channels sections as shown in figure 2.8 and an average and standard deviation of the channel signal was calculated.

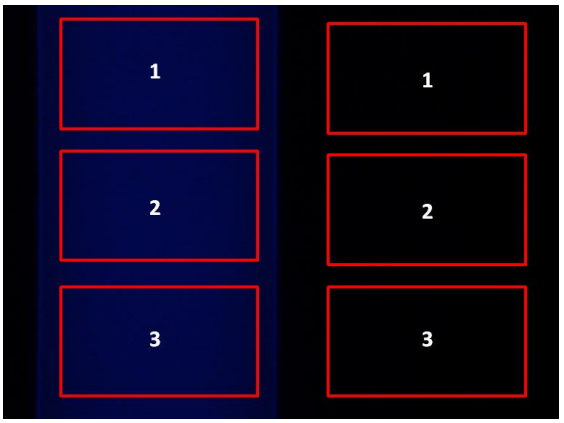

FIGURE 2.8: Representation of the sections measured during image analysis.

Chapter 3

Results

In order to optimize the microfluidic assay, different aspects were taken into consideration. Firstly, molecule surface adsorption was tested on two different surfaces: glass and PDMS. Molecule incubation parameters such as incubation time, molecules concentration and flow rate of incubation were tested. Reductions in reagents, total assay time, increase in the limit of detection and the sensitivity of the system were the main concerns in the selection of the final values used for each parameter. Blocking methodology was selected after experimentation with different blocking molecules and interaction between the system molecules was also tested in an effort to reduce the unspecific signal of the assay. All the protocols used for the optimization experiments possess a final detection step which often made use of a fluorophore for light emission. A fluorescence microscope was used for the capture of fluorescence signal. The acquisition parameters of the microscope were investigated in order to determine the relationship between gain, gamma, exposure and signal. The relation between the number of molecules on the surface and the signal intensity was assessed by performing a series of spotting assays with different antibody concentrations. Calibrations curves were made for three detection methodologies (fluorescence, chemiluminescence and colorimetry). Finally the device was integrated with an a-Si:H (Amorphous silicon) photodiodes for the acquisition of transmittance from the colorimetric assay.

3.1 Surface adsorption

3.1.1 Glass vs PDMS

Glass and PDMS were both tested as substrates for molecule incubation. Even though the devices channel (walls and top) were made from PDMS, the bottom of the channel (which is sealed after the soft-lithography step) can be sealed with either substrates. Both substrates were oxidized during the sealing process. The oxidization of the surfaces changes its properties as described in section 2.2.1 - Microfabrication.

Therefore, mouse IgG-FITC was incubated under the same conditions in both devices and the results measured in a fluorescence microscope - Figure 3.1.

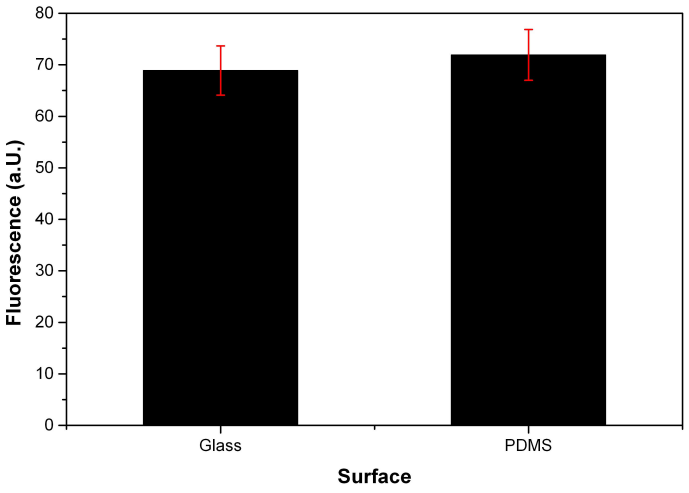

FIGURE 3.1: Fluorescence intensity results measured in the fluorescence microscopy for incubated IgG-FITC both on devices with glass and PDMS as substrate.

Through the observation of figure 3.1 it is reasonable to say that there is little difference in antibody adsorption to either substrate since the fluorescence signals and standard deviations of both assays are similar.

3.1.2 Capture Antibody Concentration

The most suitable capture antibody concentration for the assay in terms of antigen capture efficiency and reagent saving was accessed by constructing two different calibration curves. First curve consisted of incubating a monoclonal mouse antibody conjugated with FITC inside the microfluidic channel in different concentrations plus a final washing step to remove unbound molecules. Fluorescence signal was determined from pictures taken in a fluorescence microscope. For the second curve monoclonal mouse antibody unlabelled was incubated in in different concentrations followed by incubation of BSA conjugated with FITC. Results are presented in figure 3.2. FITC molecular weight is approximately 390 daltons. Even though each labelled antibody as 3 to 6 FITC molecules the extra molecular weight is negligible when compared to the antibody (150kDa). Therefore FITC molecular weight was not taken into account in the concentration calculation.

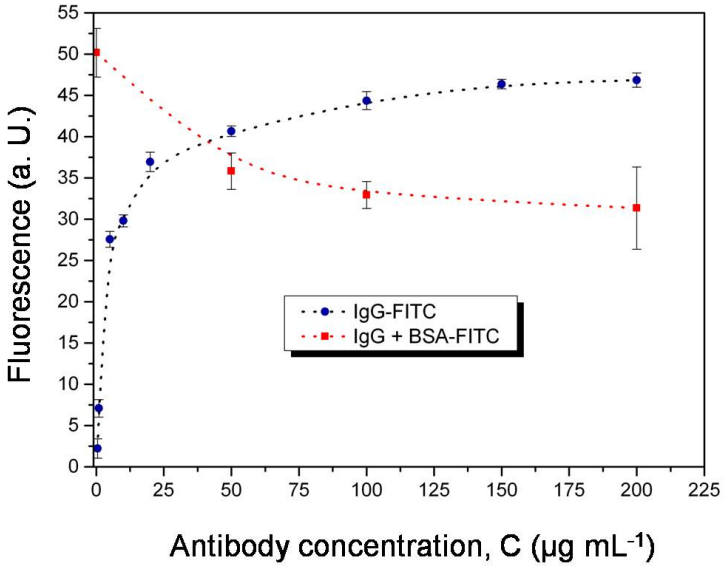

FIGURE 3.2: Fluorescence curve for FITC labelled monoclonal mouse IgG (blue) and for unlabelled mouse monoclonal IgG + BSA-FITC (red).

There is an increase in fluorescence signal when increasing the concentration of IgG-FITC - blue curve from figure 3.2 - reaching a plateau around 100 µg mL^{-1}. This same trend is confirmed by the second curve in which BSA-FITC (constante concentration) is incubated after the channel is coated with unlabelled IgG (varying concentration) -

red curve. Because of the IgG incubation, the channel has less free space for the BSA-FITC to adsorb making the fluorescence signal decrease with the increase in the IgG concentration used. This decrease in signal also reaches a constant value around 100 μg mL^{-1}.

3.1.3 Incubation time and flow rate

Various incubation times and flow rates were tested for the antibodies in order to minimize the assay time and still ensure a reasonable surface coverage of the microchannel.

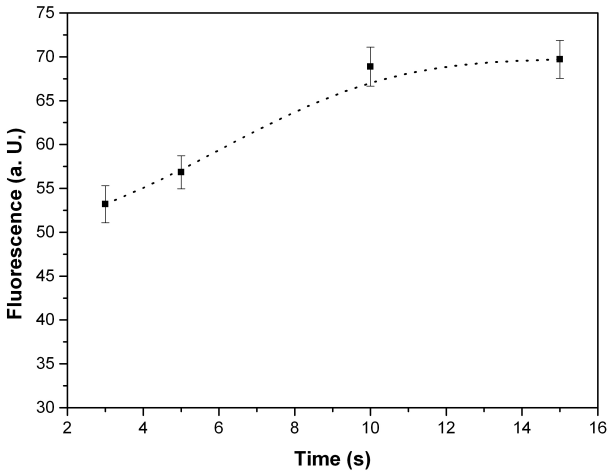

FIGURE 3.3: Fluorescence signal for the incubation of 100 μg mL^{-1} of IgG-FITC in 4 experiments varying the antibody solution incubation time.

Just as for the antibody concentration, incubation time also seems to show a plateau after 10 minutes of incubation. The incubation time for the antibodies incubation was then set at 10 minutes.

For the flow rate, the results are shown in figure 3.4. Flow rate of incubation should ideally be as low as possible in order to save reagent and at the same time not to disrupt the system (by removing molecules from the channel surface). Nevertheless, during the incubation, antibodies bind to the surface lowering the flowing solution concentration of antibody. Therefore the flow rate should be high enough to ensure constant renovation of molecules and keep the flowing solution concentration close to the initial concentration. Knowing the dimension of the channel (20x300x10000 μm), the volume was calculated

($0.06mm^3$). With a flow rate of 0.5 µl min^{-1} and a volume of the channel of 0.06 µl, the channel solution is totally renewed about 8.3 times per minute, making an average residence time inside the channel of 7.2 seconds.

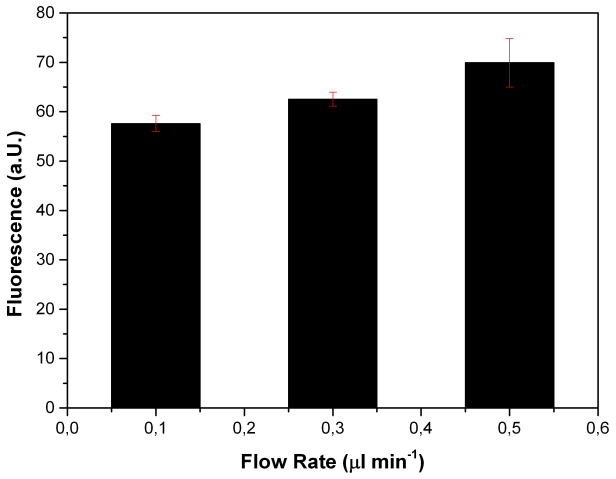

FIGURE 3.4: Fluorescence signal for the incubation of 100 µg mL^{-1} of IgG-FITC in 3 experiments varying flow rate at which the solution was incubated inside the microchannel.

3.2 Blocking Methodology

The blocking step optimization becomes one of the most important steps when the system's sensitivity and limit of detection improvement are the ultimate goal. Different blocking molecules were tested in order to evaluate antibody affinity to the blocking agent and blocking efficiency with the goal of reducing the assays control signal and minimizing non-specific bindings.

3.2.1 Blocking molecule of choice

For the blocking experiments BSA and salmon sperm DNA were tested as blocking agents using chemiluminescence as a detection method. PSA specific antibodies were used to access the affinity between these and the blocking molecule. The results are presented in figure 3.5. By the analysis of the results in figure 3.5 it is reasonable to say

the emt-PSA antibody either possess a very low binding affinity to both blocking agent, or the blocking of the surface was not completely assured by the blocking molecules. SSDNA (salmon sperm DNA) and BSA seem to show a similar blocking efficiency, with BSA showing a lower signal for the experiment with f-PSA antigen. This may reflect a better blocking efficiency or lower affinity of the antibody to the BSA when compared to the SSDNA.

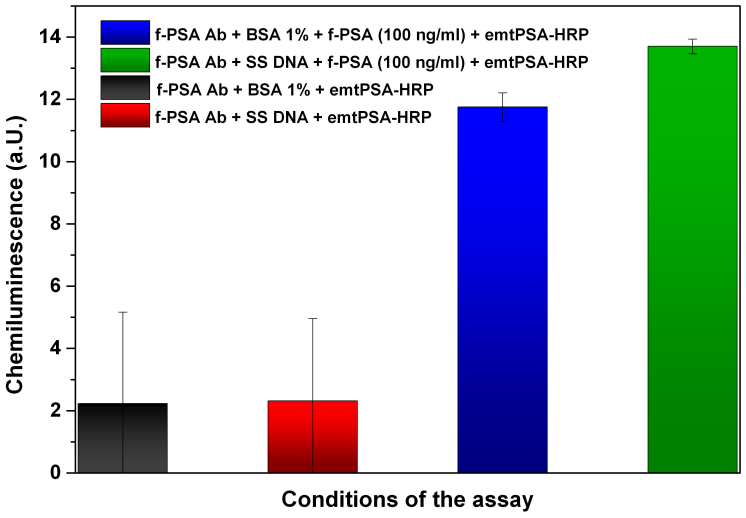

FIGURE 3.5: Chemiluminescence signal for 4 different conditions in a sandwich assay with PSA specific antibodies. (note: SSDNA stands for salmon sperm DNA)

A set of control experiments was performed in order to validate the signals acquired for the blocking experiments. All the molecules were incubated in a microchannel individually and their chemiluminescence signal measured as proof of concept for the blocking experiments - Figure 3.6.

The emt-PSA HRP incubation presents a high signal just has expected since there was no blocking of the surface and all the labelled HRP antibody molecules bound to the surface leaving the channel covered with HRP. The BSA and SSDNA covered channel showed almost no signal at all since there was no HRP present of the channel for the substrate (luminol) degradation.

Flowing detector antibody in the BSA blocked channel showed a higher signal then the SSDNA blocked channel. However the difference is no bigger than the standard deviation for the BSA blocked channel (1 a.U.).

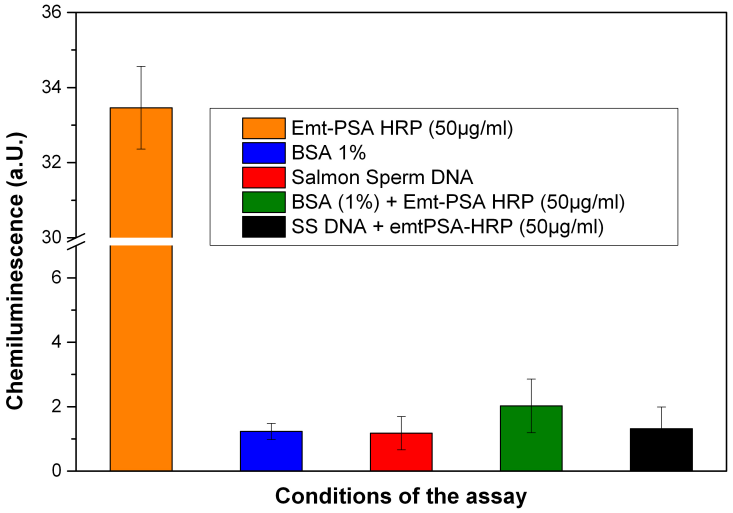

FIGURE 3.6: Set of controls experiments for the sandwich chemiluminescence assay.

All in all there a similar efficiency in the blocking with both methods however small differences are worth notice. Since the SSDNA presents a higher signal for the sandwich experiment with 1 µg mL^{-1} of f-PSA than when blocked with BSA (Figure 4.5) and at the same time, presents a lower signal when only blocking agent and detector are incubated (Figure 3.6) we can assume some kind of capture antibody-SSDNA interaction. A reduction in the blocking efficiency is ruled out since the capture-blocking-detector experiment (black and red columns-Figure 3.5) show the same blocking efficiency for both methods. Therefore weak interactions between antigen or detector antibody with the SSDNA may be the cause for this slightly higher signal in the full sandwich experiment. This interaction between SSDNA and the other systems proteins could be confirmed with a electrophoretic mobility shift assay. If there is interaction between these molecules a reduced mobility should be observed in the SSDNA migration through the gel.

Casein was also tested as a blocking agent along with different concentration of BSA and a 50-50 mixture of 2 % BSA and 100 µg mL^{-1} of casein - Figure 3.7. The experiment comprised only two incubation steps. A blocking step with the different solutions and the incubation of detector antibody (IgG-FITC) followed by a final washing with PBS to remove unbound molecules. A reduction in signal is observed with the increase in the concentration of BSA although this is accompanied by an increase in the standard deviation. Casein alone showed a much lower blocking efficiency when compared to BSA.

The mixture between the two blocking agents presents a blocking efficiency similar to the BSA assays although still less efficient than 4 % BSA alone. The interaction between both proteins (casein and BSA) may not favour the binding of either to the channel surface.

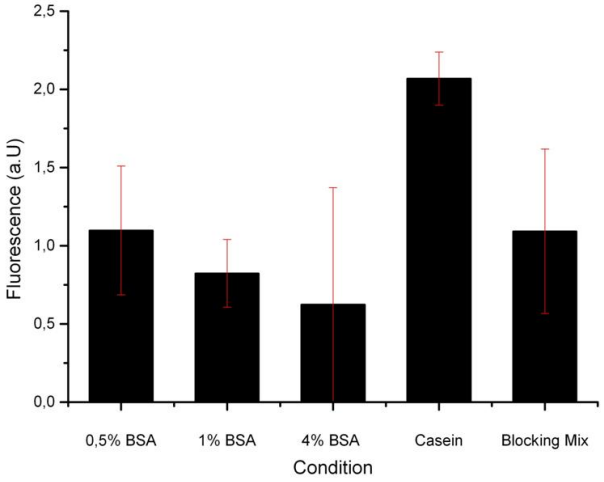

FIGURE 3.7: Testing different BSA incubation conditions and casein blocking efficiency. A mixed solution with 50 % BSA at 4% and 50 % Casein at 200 µg mL^{-1} was also tested as blocking solution.

3.2.2 Blocking parameters

Taking into account the results from the blocking experiments BSA was chosen as the blocking methodology. Therefore incubation time was optimized to try to reduce the total assay time - Figure 3.8. The assay consisted of 2 incubation steps. Blocking step varying incubation time and running detector antibody (IgG-FITC) followed by a final washing with PBS to remove unbound molecules.

From figure 3.8 it can be seen that 5 minutes of incubation time seems to show the most efficiency of the 3 assays. The difference between 1 minute incubation and 3 minutes incubation is negligible do to the high standard deviation presented by the 3 minute assay. The 5 minute incubation however presents a distinct indication of better blocking than the remaining 2 assays. 5 minutes incubation was chosen for standard time of incubation for the 4 % BSA solution.

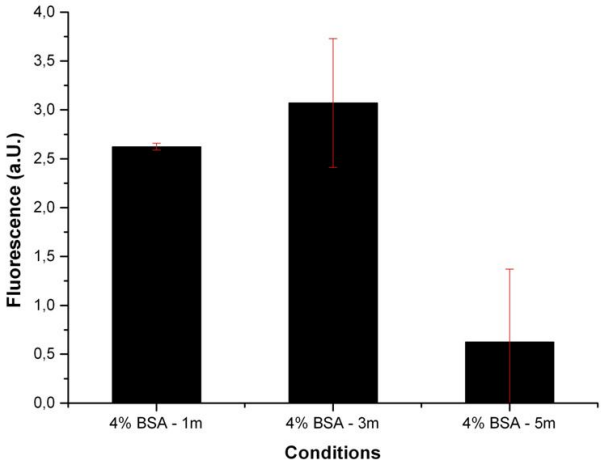

FIGURE 3.8: BSA incubation time experiment. Constant concentration of BSA (4 %) was incubated for 3 different time periods and IgG-FITC flown afterwards for detection.

Finally, the blocking system was tested with a goat-IgG - blocking - αgoat - IgG-FITC assay varying the concentration of the blocking agent of choice (BSA) and the using the previously defined parameters (10 minutes incubation time for antibodies and 5 minute incubation time for BSA at 0.5 µl min^{-1}). - Figure 3.9. This evaluated the blocking efficiency on a surface already coated with an antibody.

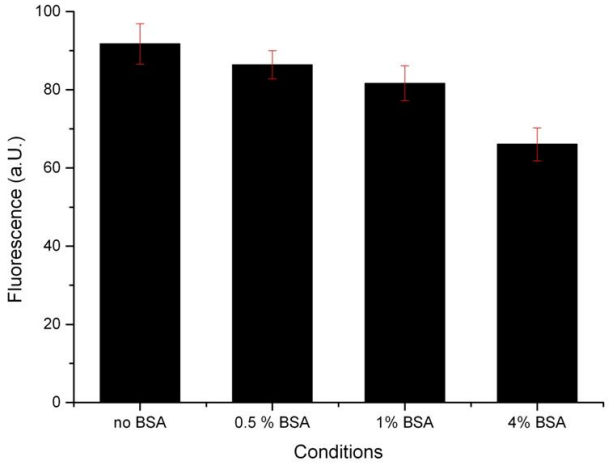

FIGURE 3.9: Testing different BSA incubation conditions with goat-IgG - blocking - αgoat - IgG-FITC assay.

As expected the 4 % BSA showed the lowest signal indicating the best blocking performance justified by the higher number of molecules which will increase the binding

affinity to the surface.

3.3 Washing conditions and PSA antibodies' controls

3.3.1 Washing conditions

Although a final washing step is necessary to remove all unbound molecule and ensure that the signal measured is referent to the amount of free PSA in the assay the flow rate at which PBS (washing solution) is ran in the channel does not seem to cause much variation in the signal - Figure 3.10. This experiment comprised the incubation of free PSA capture antibody, a blocking step and the incubation of emtPSA-FITC antibody. No free PSA was incubated in the channel. The control followed the same protocol but did not include the final washing step. The washing step had a duration of 1 minute.

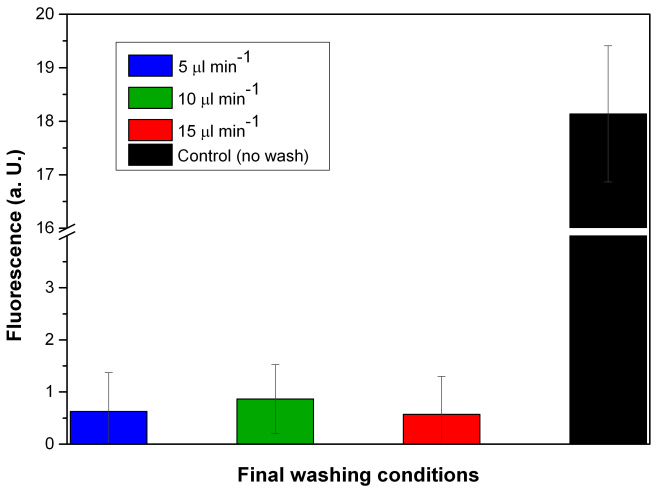

FIGURE 3.10: Washing conditions tested on the final washing after capture-blocking-detector incubation.

These results show the lowest stringency wash (5 µl min^{-1}) is enough to remove all unbound or non-specifically bound molecule inside the microchannel. Therefore there is no need to increase the stress inside the channel with higher flow rates. At the same time a lower flow rate means less reagent loss.

3.3.2 PSA antibodies' controls

Another important aspect of an optimization is to have a set of controls for the antibodies used in the system established. These controls ensure that the molecules used are working as predicted and help to uncover any unspecific interactions that may arise from the combination of different molecules on the system. Results for the PSA Antibody controls are presented in figure 3.11. The antibodies were incubated individually in each experiment and in different combinations to allowed for a complete system study. A washing step was performed at the end of each experiment before luminol was ran in the channel for the detection under the microscope. The previously defined values for the molecules incubation time, flow rate and concentration were used.

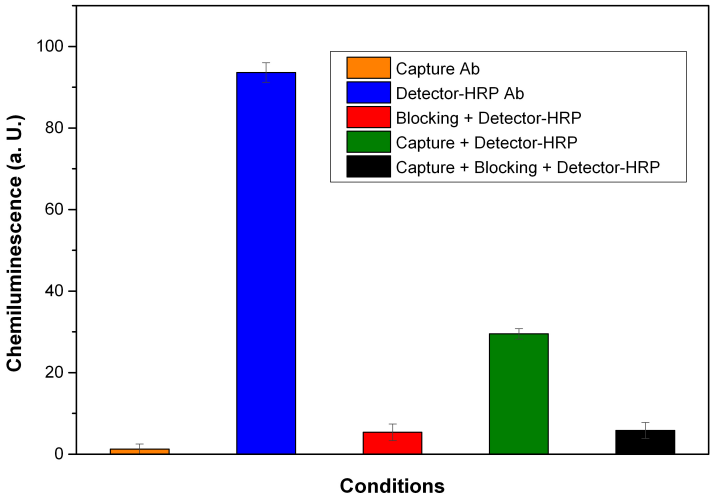

FIGURE 3.11: Control experiments for the PSA antibodies.

3.4 Microscopy fluorescence data acquisition

For fluorescence experiments image acquisition parameters must be defined to optimize the signal read (Figure 3.13). FITC molecules have a decay ratio of fluorescence associated with said molecules exposure to excitation fluorescence light. The purpose is to increase the signal per molecule ratio as much as possible keeping the bleaching of the FITC molecules at minimum. With gain there is an introduction of digital distortion to the image in order to increase the overall fluorescence measured in the image acquired.

It is also important to have in mind that to much signal amplification may result in over exposure and loss of signal quality. In figure 3.12 it is clear section B imaging was acquired with the wrong parameters. There is a clear cut off on the Z axis of the values because they reached the maximum value allowed in the bit system (255). This makes it impossible to distinguish the signal variation and more importantly, caps the concentration measurements at a value lowered then our actual detection range.

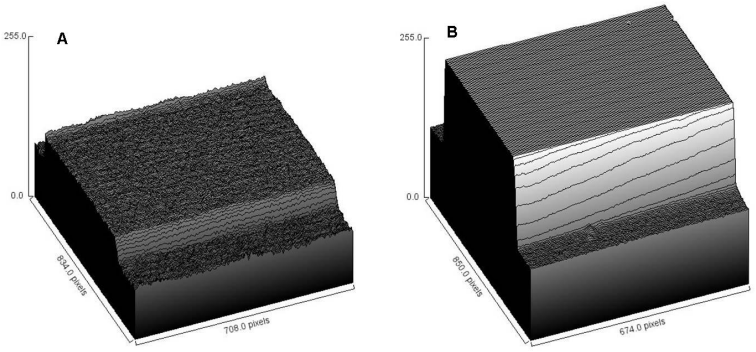

FIGURE 3.12: Comparison between a control (A) and an overexposed (B) image of a microchannel incubated with FITC labelled antibodies.

There is also a possibility of finding a constant to calibrate signals acquired with different exposition conditions. A set of pictures were taken of the same microchannel at different acquisition conditions for the construction of the graph in figure 3.13. This depicts the relationship between the acquisition variables and the signal captured.

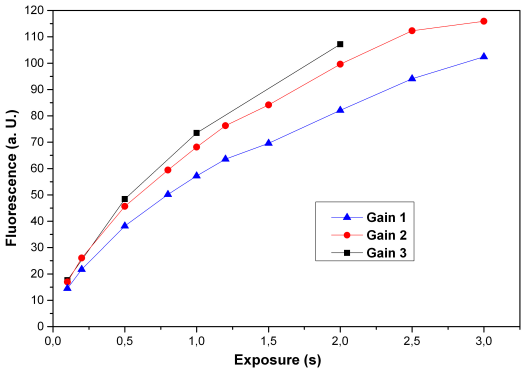

FIGURE 3.13: Microscopy fluorescence data acquisition. The data for the three curves was acquired at fixed gamma (0.6). Within each curve gain was constant (1, 2 and 3) and exposure was varied from 0.1 to 3 seconds.

3.5 Colorimetry detection optimization

Colorimetry assay required further optimization due to the intra-experimental variations of the absolute values of absorbance. The TMB used was a Blotting Substrate Solution from western blot assay. Unlike the ELISA TMB solution this western blot TMB develops a permanent, insoluble dark blue reaction product which precipitates inside the microchannel. This precipitation leads to a difference in signal depending on the channel area measured. This variation in signal along the channel is shown in Figure 3.14. Measurements were taken in three different areas of the channel during a period of 7 minutes in order to evaluate signal variation. The measured values were normalized to the absorbance value measured from an empty PDMS microchannel.

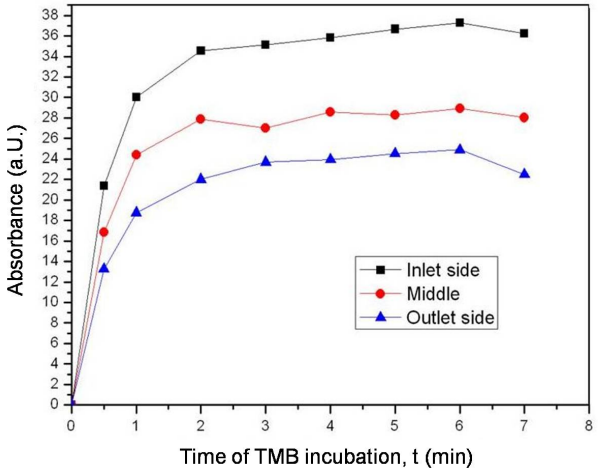

FIGURE 3.14: Measurements of TMB product along the microchannel. Inlet side- 2mm away from inlet; middle - 5mm away from inlet; outlet side 2 mm away from the outlet.

3.6 Spotting Assays

Microfluidics devices have shown in recent year to be capable of providing a cheaper, faster and portable system for the performance of miniaturized immunoassay. These devices are developed with the goal of fabricating a PoC device for the analysis of various metabolites performing all the top-bench tasks bearing the same reliability in a single portable chip. For the purpose of multiplexing, spotting has been used in order to provide the microfluidic system with selective areas for different metabolites in an

immunoassay context. However spotting can also be used has a tool for the study of antibody behaviour on different substrates providing information for the analysis of flow incubated molecules on a microchannel.

With spotting assay is easy to know the total amount of antibody on the channel surface due to the possibility of handling the amount of droplets spotted, knowing that each droplet has a volume of 0,56 picoLiter. This allows for the calculation of antibody total amount, surface density and signal per molecule. In this section the results for 3 spotting assays are analysed and discussed.

3.6.1 Spotting Concentration Curves

Pictures of all spots were taken and fluorescence signal was measured. The fluorescence signal correlates to the concentration of antibody on each spots. Therefore a curve of antibody-FITC concentration versus fluorescence signal was drawn. Keeping in mind the signal measured is bit-dependent and ranges from 0 to 255, the variation in the acquisition parameters (namely exposure) as referred previously was necessary to ensure the images acquired would output a reasonable value for analysis avoiding overexposure of the signal. Over exposure would deviate the results, as this would mean loss of sensitivity in the higher concentrations. However, the variation is restricted to inter-experimental assays so that the values in each experiment are comparable and fit to a curve as seen in figure 3.15. Spotting experiments 1 and 2 results were acquired with 0.2 seconds of exposure. Experiment 3 was imaged with 1 second of exposure.

Although there is an inter-experimental exposure difference in this data, is it important to see that the data follows the same trend varying the slope of the increments. This is due to the difference in exposures. By comparing the signal for the 100 $\mu g\ mL^{-1}$ we can easily understand that with a 1 second exposure the results for 500 $\mu g\ mL^{-1}$ spots in the first and second assay would have suffered overexposure.

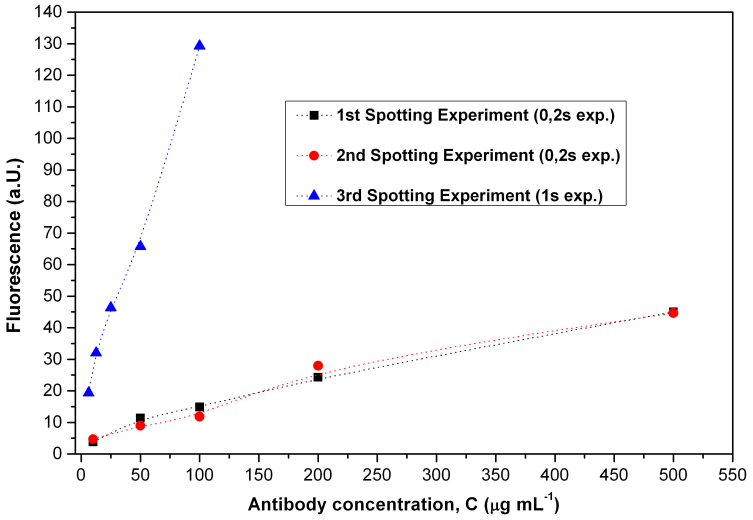

FIGURE 3.15: Fluorescence curves for the 3 spotting experiments. Antibody-FITC concentration used versus Fluorescence signal.

3.6.2 Antibody surface density

The area of each spot was measured and the density of antibody on the spot calculated. The difference in spot size makes it impossible to have a linear relationship between the molecules density and the antibody concentration used. This can be observed in picture 3.16. The inset bar graph has represented every spot's size.

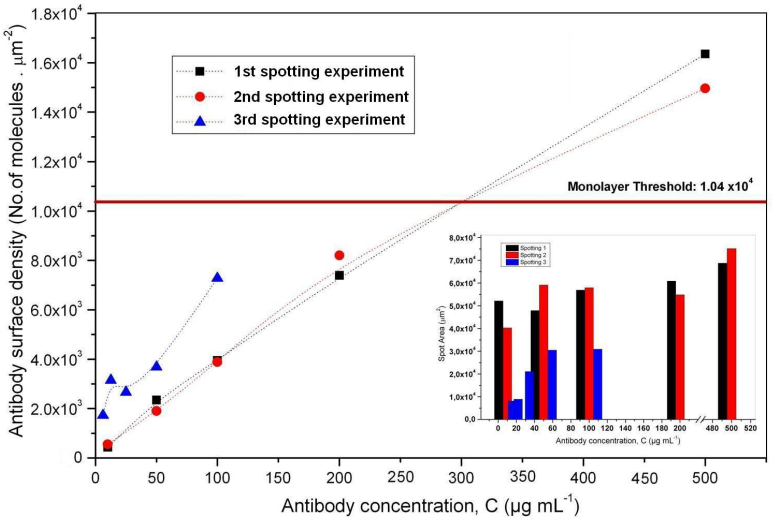

FIGURE 3.16: Graphic presents the antibody surface density for each spot measured versus the antibody concentration used. The inset graph shows the area measured in each spot. The red like is the monolayer theoretical threshold.

The theoretical monolayer threshold was calculated based on the area occupied by the average antibody (calculated by assuming an hydrodynamic radius of 5,5 nm) and its respective molecular weight (150 kDa).

There was a distinct relation between spot size and the concentration used, clearly observed in the third experiment. This experiment comprised a difference in protocol when compared to the first and second. The antibodies were diluted in PBS with 5 % glycerol. This was done in order to slow down the evaporation (even though humidity was set to 75 % inside the nanoplotter) of the droplets due to the very small volumes used. This allowed a more homogeneous distribution of the antibodies throughout the spot arena as it can be seen in figure 3.17.

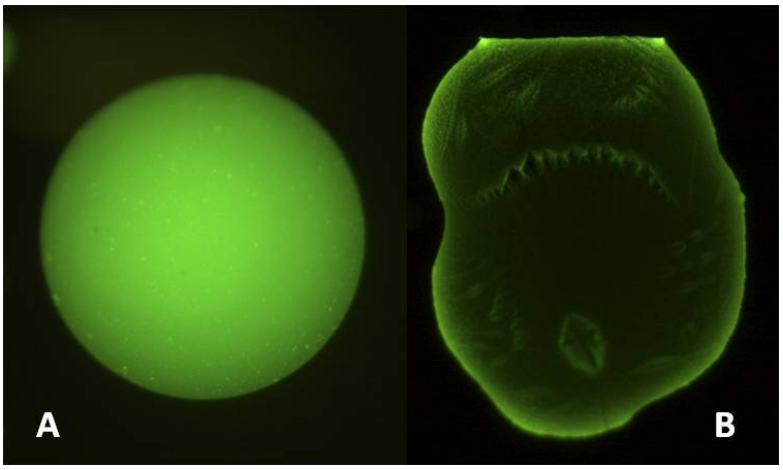

FIGURE 3.17: Spot experiment images. A - Spot from the third experiment (antibody diluted in PBS 5 % glycerol). B - Spot from the second experiment (antibody diluted in PBS).

3.6.3 Fluorescence signal per molecule

A more interesting trend is observed when antibody surface density is plotted against signal per molecule.

The spotting experiments allowed for a quantification of the number of molecules on the surface since the experiment required total control over the spotted volume and the droplet area occupied could be easily measured on the microscope with the appropriate calibration. A comparison between the number of pixels measured by ImageJ in each droplet picture was compared to the number of pixels measured for the channel width

(300 µm). Knowing the total number of molecules on the spot, surface density was calculated. Total amount of signal measured in the spot was divided by the number of molecules present in each spot and plotted against the molecules surface density - figure 3.18.

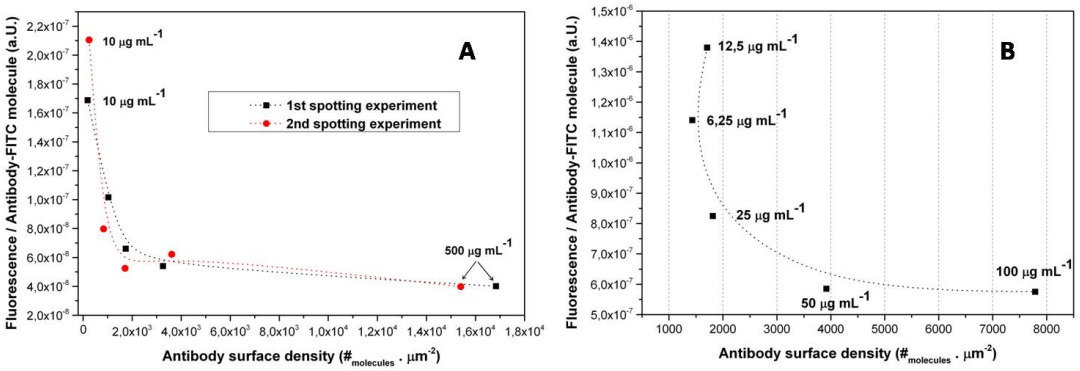

FIGURE 3.18: Antibody-FITC surface density vs fluorescence signal per molecule. A - Spots from the first (black) and second (red) experiment. B - Spot from the third experiment.

As it is observable in figure 3.18, this signal is dependent on the exposition conditions used for imaging therefore experiments 1 and 2 are separated from the third.

3.7 Detection calibration curves

After optimizing the microfluidic device and the assay detection curves were elaborated in order to evaluate the sensitivity of the different detection methodologies. Fluorescence, chemiluminecence and colorimetry assays were performed using the previously defined parameters for the molecules incubation. For fluorescence a FITC labelled emtPSA antibody was used as detector antibody. For the chemiluminecence and colorimetry the same antibody was used but labelled with an HRP enzyme instead of FITC molecules. The experiments for the acquisition of the data points were all performed on the same device to reduce inter-experimental variation and using the same antibody dilutions. Free PSA solution varied in concentration. Linear fit for each calibration curve was calculated using Origin 9 analysis tools.

3.7.1 Fluorescence curve

For the elaboration of this curve, three different areas of the channel were measured and a mean and standard deviation calculated for each concentration point. Full graphic presented is in figure 3.19 in a graphic.

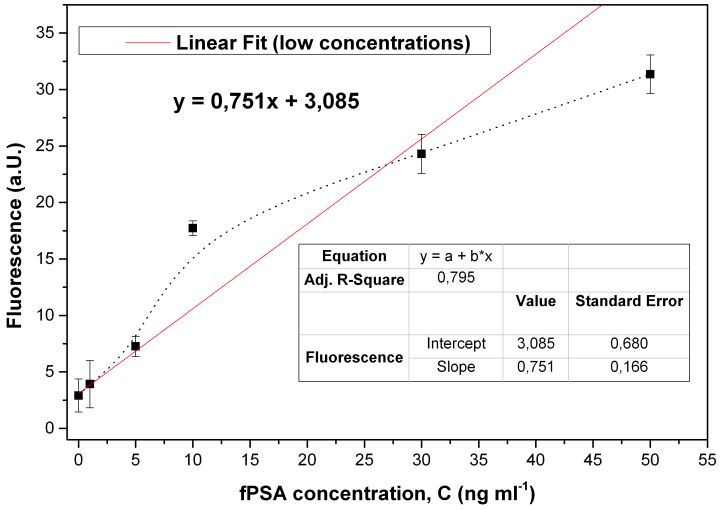

FIGURE 3.19: Fluorescence calibration curve using a full sandwich fPSA assay with fluorescence detection method. A linear fit curve was calculated for low concentrations ($\leq$ 50 ng mL^{-1}). The dotted line is just an eye guideline.

Having in mind the goal of defining an LoD and LoQ for our system decreasing values of concentration were tested until there was no clear difference between the control (no analyte) and the lowest concentration tested. The linear fit, even though with a low R^2, provide us the slope of for the low concentrations. For this goal only analyte concentrations under 50 ng mL^{-1} were consider for the linear fit calculation. The reason for this is because the systems signal to concentration response is not linear due to signal saturation and also do to the modifications made on the signal by manipulations of the imaging parameters (gains, exposition, gamma). For this reason, a polynomial fit would be the most appropriate for the graphic's characterization. However for a polynomial fit, a larger range of concentrations would need to be measured and included. Since the goal is access LoB's, LoD's and LoQ's, focus was made on the lowest concentrations and a linear fit adjusted to these.

3.7.2 Chemiluminescence curve

The chemiluminescence curve was projected with the same conditions used for the fluorescence. Three images were taken from the channel and mean and standard deviation calculates.

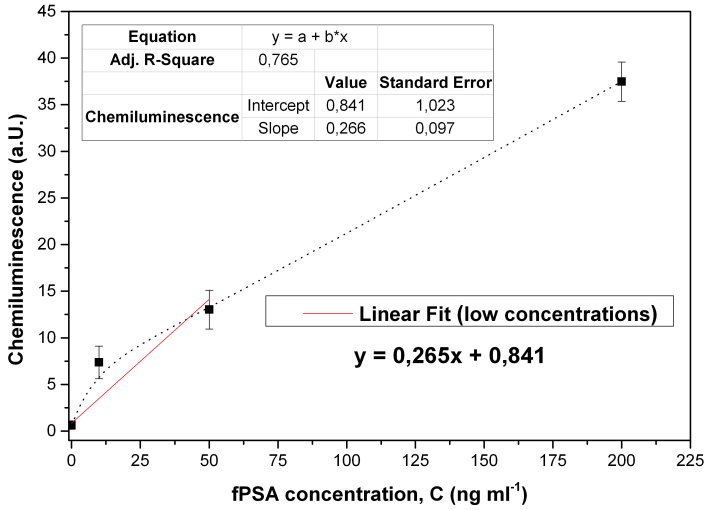

FIGURE 3.20: Chemiluminescence calibration curve using a full sandwich fPSA assay with HRP labelled detector antibody and luminol as detection substrate. A linear fit curve was calculated for low concentrations ($\leq$ 50 ng mL^{-1}). The dotted line is just an eye guideline.

The same protocol used for the fluorescence analysis was applied to the chemiluminescence results. Preliminary experiment lead to the belief that even though chemiluminescence was an accurate method, it did not possess enough sensitivity for the concentrations of interest (1-10 ng mL^{-1}). Higher concentrations were then measured however the experiment for 100 ng mL^{-1} failed and the result was treated as an outlier due to the fact that in the imaging process there was no signal.

3.7.3 Colorimetry curve

The colorimetry curve was measured in two different devices. In the microscope, just as the fluorescence and chemiluminescence assays, and using the bottom light source at maximum intensity and fully open condenser, pictures were taken of the transmission

plus a control (clear channel) in order to calculate the absorbance of the TMB reaction product. Results presented in figure 3.21.

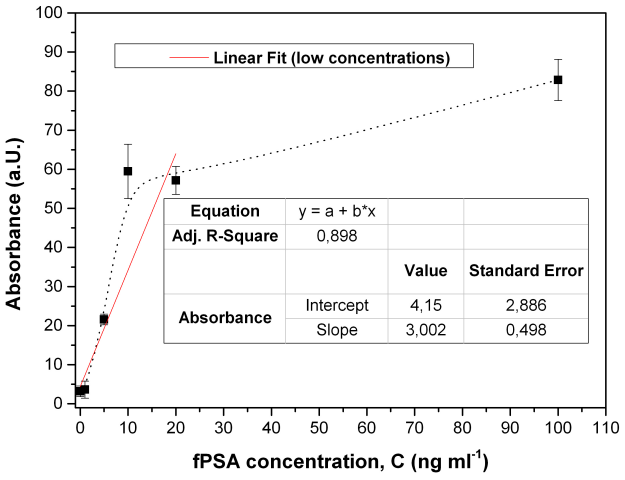

FIGURE 3.21: Colorimetry calibration curve using a full sandwich fPSA assay with HRP labelled detector antibody and TMB as detection substrate. Signal detection was measured through a microscope. A linear fit curve was calculated for low concentrations ($\leq$ 50 ng mL^{-1}). The dotted line is just an eye guideline.

After all the measurements, transmission results were converted to absorbance by normalization with the maximum signal captured through a clear channel. This maximum signal would correspond to the absorbance minimum. Assuming this, all other acquired measurements (including the blank) were subtracted to this maximum signal value. This difference between the two represents the amount of signal absorbed by the TMB precipitate on the channel.

The colorimetry assay was also measured in a-Si:H photodiodes. The microfluidic device was aligned on top of a PCB wirebonded to the PD's. This PCB plugged to a picoammeter for current measurements. On top of this assembly, a light source is placed directly on top of the photodiodes, and the amount of light transmitted through each microfluidic channel to the PD is measured in current density - Figure 3.21.

3.7.4 Limits of detection

After linear fit was performed, line parameters and standard deviations were used for the calculation of the LoB (limit of blank), LoD (limit of detection), LoQ (limit of quality).

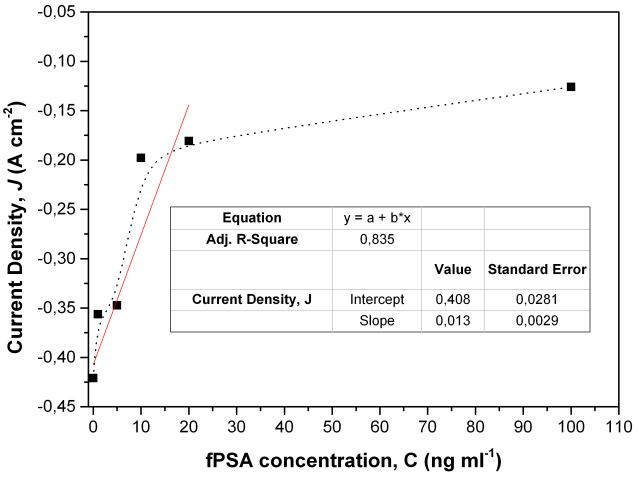

FIGURE 3.22: Colorimetry calibration curve using a full sandwich fPSA assay with HRP labelled detector antibody and TMB as detection substrate. Signal detection was measured through PD's connected to a picoammeter. A linear fit curve was calculated for low concentrations ($\leq$ 50 ng mL^{-1}). The dotted line is just an eye guideline.

The formulas used for the calculation of all three parameters are listed below:

- LoB = Mean$_{blank}$ + 1.645 * (SD$_{blank}$)
- LoD = ((3.3 * SD$_{blank}$) - intercept) / slope
- LoQ = ((10 * SD$_{blank}$) - intercept) / slope

Following the previous formulas, these parameters were calculated for the three detection methodologies and results are presented in table 3.1.

TABLE 3.1: Calculated values for LoB, LoD and LoQ for the three detection methods. Colorimetry assay was measured both in microscope (M) and photodiodes (PD).

	Parameters		
	LoB (measument units)	**LoD (ng mL^{-1})**	**LoQ (ng mL^{-1})**
Fluorescence	5.31	2.30	15.32
Chemiluminescence	1.38	2.44	13.81
Colorimetry (M)	5.41	0.10	3.10
Colorimetry (PD)	-0.421	0.062	0.187

All values used for these calculation came from the results used to build figures 3.19, 3.20, 3.21 and 3.22 and formulas in 3.7.4. Nevertheless all the data for each calibration

curve was performed on the same day and on the same device. Inter-day and inter-device experiments should be performed in order to assess more reliable detection limits.

3.8 Integration with photodiodes

For the integration of the microfluidic device with photodiodes, a PCB was milled in order to allowed for the microfluidic device to slide in and minimize the distance between the photodiodes (already attached in a pocket previously made on the PCB) and the microchannel area to be measured.

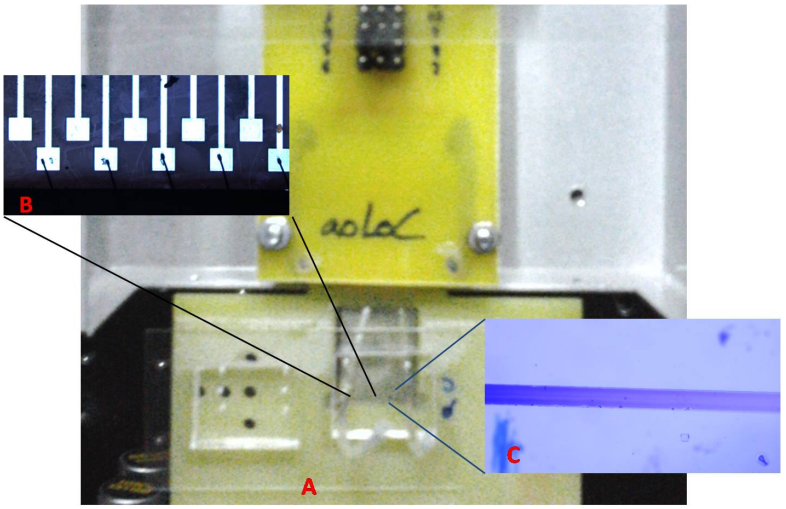

FIGURE 3.23: Assembly of PCB with wirebonded photodiodes with a microchannel aligned on top of the PD's. A - Microfluidic device on top of the PD's; B - PD's microscopy photograph; C - Microchannel with TMB precipitate microscopy photograph.

The previous figure shows the assembly required to make measurements of microfluidic assays on PDs. These PDs are 100 x 100 µm in size, while the microchannel has a 300 µm width, ensuring that all of the diode gets covered by the microchannel. This is particularly important for the colorimetry detection, since no light should reach the PD without going through the microchannel to ensure the absorbance ratio of the TMB precipitate is taken into account.

Chapter 4

Discussion and Conclusions

4.1 Discussion

4.1.1 Optimization steps

Glass was chosen as the substrate of choice for the following reasons: the antibodies presented roughly the same adsorption efficiency as in PDMS (the other possibility as substrate); it provided an easy to slide base for the integration of the device with a detection platform. This allows the assay to be performed in the same substrate which will directly slide and align with the PD's for integrated detection.

The capture antibody concentration was tested having in mind two goals: full surface coverage and minimum concentration required to do so. The results presented in figure 3.2 show the fluorescence signal for increasing concentration of IgG on the channel surface. A reverse experiment is also plotted in which channel was first covered with unlabelled IgG and then BSA-FITC was flown. Around 100 $\mu g\ mL^{-1}$, the fluorescence signal reaches a plateau. This is proof that the surface gets saturated and molecules are no longer able to adsorb ending up being washed out of the channel. Therefore 100 $\mu g\ mL^{-1}$ of antibody was defined as the standard concentration for the capture antibody incubation solution. The presence of such a high fluorescence signal in the BSA-FITC experiment even after full surface coverage by IgG is due to the fact that BSA (66.5 kDa)

is several times smaller then IgG (150 kDa) and fills the spaces left between antibodies on the surface. This is ideal as it provides a full coverage of the surface.

Incubation time for antibodies was set at 10 minutes since this time frame presented a similar fluorescence signal to the 15 minutes incubation experiment. However the aim is to reduce time and reagent.

The flow rates were tested and the highest (0.5 μL min^{-1}) was chosen since it presented the highest signal after 10 minutes of incubation of IgG-FITC. Higher speed were not tested since the goal was to cause the least disturbance on the system. The flow rates tested aimed at refreshing the antibody concentration inside the channel as the molecules start to adsorb to the channel surface. At 0.5 μL min^{-1} the whole microchannel volume is refreshed every 8.3 seconds. This means that over the course of 10 minutes of incubation the channel will be filled with a solution of 100 μg mL^{-1} of antibody about 72 times.

BSA and SSDNA presented similar efficiencies in terms of blocking. However in the target specific experiment (figure 3.5 - blue and green) BSA demonstrated a slightly better efficiency. This difference may be due to a better blocking efficiency of the BSA, or the SSDNA demonstrating some unspecific interactions to antibodies due to intermolecular forces: ionic interaction; hydrogen bonding; hydrophobic interactions. This leads to the use of BSA as blocking agent.

A set of control experiments is presented for the blocking methodology as a proof of concept for the blocking in the developed assay - figure 3.6. The emtPSA-HRP experiment obviously presented the highest signal since it did not have any molecules restricting the adsorption to the channel surface. The BSA and SSDNA channels were not incubated with any detection molecule and as such they only presented background equivalent signal. Running the detector after the two blocking molecules proved the efficiency of the blocking methods, as seen in the huge signal reduction when compared to the non blocked channel.

Further ahead in the project came the need to test a different blocking agent - casein - due to its reputation as a excellent blocking agent. However the results on figure

3.7 show that 4 % BSA alone is a better channel blocker than any other methodology, including a 50-50 % mixture of 200 µg mL^{-1} and 4 % BSA.

The blocking solution incubation time was also assessed as shown in figure 3.8. The 5 minute incubation experiment presents the lowest signal therefore it was the chosen time for the BSA incubation in the sandwich assay. Other incubation time frames could have been tested but the 0.7 a. U. signal is practically equivalent to background noise, therefore there is no need to increase the assay time further.

The need for a blocking agent and its effect on a fully covered surface was tested - Figure 3.9 - with various BSA concentrations. The results clearly indicate there is a great need to block the surface with a smaller molecule even after full surface coverage by a capture antibody.

The washing solution flow rate was tested to evaluate its efficiency. Results show no relevant difference between the three flow rates tested. Because of this, the lowest flow rate was chosen as the standard washing speed as there is less reagent waste and less stringency applied to the system.

PSA antibodies control experiments - figure 3.11 - were made to ensure the reliability of the system's output. This is a proof of concept for our sandwich system. The controls demonstrated a good reliability of the system. The incubation of capture antibody demonstrated no signal at all since there was no HRP inside the channel. The incubation of the emtPSA-HRP directly on the surface exhibited a very high signal since the channel was fully covered with HRP labelled antibody. The blocking of the surface with BSA previously to the incubation of the detector antibody proved to be efficient minimizing the binding of the detector antibody in the channel. Incubating capture antibody followed by detector, without a blocking step, demonstrated the importance of the blocking step by showing a higher signal than the experiment with blocking step in between the antibodies incubation. This also proves the surface was already occupied with the capture antibody, and the amount of free space for the detector antibody to bind was reduced since the signal is much lower than the experiment in which the detector was incubated on the empty channel.

The data acquisition experiments - figure 3.13 - allowed to conscientiously choose the best parameters in order to have the highest signal possible without capping our concentration limit or bleaching the fluorescence signal. The conditions chosen were 1 second of exposure, 1 gain and 0.6 of gamma. By having no gain amplification in the signal, introduction of unwanted signal distortion is avoided.

Colorimetry detection method required one extra step in the optimization process. The parameters for TMB flow and also region on the channel measure introduce variation to the final signal acquired. Therefore these were optimize in order to have the most sensitivity to the concentrations of interest (1 to 4 ng mL^{-1}). TMB was flown in the channel and signal measured in 3 different areas from 30 seconds to 7 minutes of incubation: The inlet side measured was located 2 mm away from the inlet; the middle section was 5 mm away from inlet and outlet; the outlet side was 2 mm away from the outlet. Results in figure 3.14 clearly depict a difference in the absorbance value acquired between the 3 locations. Since the substrate is enzymatically converted as soon as it enters the channel, this affects the concentration of the substrate solution that will reach the channel areas further away from the inlet and at the same time leads to an increased accumulation of product from the reaction near the inlet of the channel. Therefore it becomes important to define the exact location of the microchannel to measure as well as the time of incubation and flow rate whilst the TMB incubation. It is necessary to guarantee that each time TMB is flow, the same amount of substrate reaches the defined measurement area during the same amount of time. Ideally, the absorbance signal should be as high as possible to increase assay sensitivity. However since there is a tendency for the formation of aggregates near the holes (due to the disruption of small PDMS pieces from the punched hole) a safe distance of 2 mm was established in order to avoid interference from said aggregates formation. There seems to be a saturation of the absorbance after 3 minutes of TMB incubation at 10 µl min^{-1}. Just so these were the TMB incubation parameters established for the colorimetry substrate incubation.

4.1.2 Spotting experiments

Spotting assay comprised two goals. First, to prove the possibility of having a single channel covered with different capture antibodies in clearly defined areas. Also the concentration calibration performed allowed for the characterization of the molecules distribution on the adsorbed surface.

Even though figure 3.16 inset graph shows there is a greater homogeneity in spots size, in the first and second experiment when compared to the third, the antibody adsorption to the channel was not as homogeneous - figure 3.17. This is most likely due to the evaporation time. The third experiment solutions possess 5 % glycerol which prevent the fast evaporation of the molecules allowing for a more homogeneous adsorption to the surface.

In all three spotting experiments there is a clear tendency to have a diminished value of fluorescence per molecule when the amount of molecules on the surface (antibody surface density) increases. This is probably due to the fact that molecules packed together will end up muffing the neighbour molecules signal. It would be useful to predict the signal per molecule and use this value to calculate the surface density of molecules in the sandwich assay through the detected fluorescence signal. However an absolute fluorescence value for a single antibody-FITC can not be defined since this muffing effect will alter the signal detected depending on the same physical magnitude trying to be measured - antibody surface density. Nevertheless for the calculation of a single antibody-FITC signal, having in mind the muffling effect, the use of the lowest concentration possible would be the most correct since there are fewer molecules in the system interfering with the emitted fluorescence.

4.1.3 Detection Calibration Curves

The calibrations curves were used to try and define the limits of detection of the system as well as the system's sensitivity.

In table 3.1 the detection limits calculated for all three detection methods using the microscope are presented. Chemiluminescence presents the highest values for LoD and LoQ, however it presents a low LoB. LoB is not comparable since this is value is presented in a.U. and imaging methodologies differ for the three methodologies. This detection method seems to need the implementation of an amplification methodology that would greatly increase the signals detected. Using a biotin-streptavidin amplification system, this technique could easily become sensitive enough for the measurement of the concentrations of interest (1-4 ng mL^{-1}) mostly due to the very low LoB. Fluorescence shows LoD and LoQ similar to the chemiluminescence detection. Further optimization of this assay is required mostly to try and decrease the LoB value which would muffle the low concentration signals.

By the calculated figures colorimetry seems to be the most sensitive method. However further repetitions of the assay would be necessary to ensure this premise. The standard deviation for the blank using colorimetry detection was in fact the lowest of the three methods. Such a low SD values indicate colorimetry is most likely the most reproducible and reliable detection system.

Colorimetry measured in the microscope presents the highest slope which means that it possesses the largest signal change per analyte quantity. Slope values cannot be compared between the PD and microscope measurements because of the different magnitudes measured (current density and a.U. respectively). Nevertheless a high resolution in the lower concentration values is observable for the colorimetry detection using the PD's. This strengthens the idea of colorimetry as the most reliable method. The fact that the TMB flowing conditions can be adapted to more assertively measure different ranges of concentrations is also a positive argument in favor of colorimetry. The PD results for the colorimetry have little relevance in terms of LoD and LoQ calculation due to the fact that only one measurement was made for each concentration. This measurement is the result of a mean from the values acquired over a minute after the TMB flow was stopped. Therefore the standard deviation calculated is associated with the measuring device error (picoammeter). Another colorimetry curve was measured on the PD but

different illumination set ups were used, and therefore these cannot be used for means and SD calculations.

All in all none of the detection methods was precise enough to reach the predetermined goal of clinically relevant concentrations for the f-PSA molecule. However colorimetry seems to show great promise. A possible optimization would be the introduction of an amplification system which would greatly benefit the chemiluminescence and colorimetry detections. This indicates that enzymatic assays reveal more sensitive detection than the fluorescence method. Colorimetry can even benefit from a time based analysis to the increase in absorbance over time during the TMB incubation. A regression can be fit into the increasing absorbance values during the TMB incubation. Linear fits of these regressions with different slops can be translated into concentrations.

The microfluidic device was align on top of the photodiodes by using one of the sides of the glass against a previously made groove on the PCB. However this only provided the alignment of one axis, being the second axis align by hand with the help of a magnifying glass. The integration of the device with the photodiodes can be greatly improved by developing a simple groove to slide the microfluidic device in and instantly align the microchannel with the photodiodes.

4.2 Conclusions

Throughout this work it was demonstrated that biomolecules can be adsorbed on PDMS microchannel with a glass substrate. This allows for an ELISA to be performed in microscale under 45 minutes with minimum molecule consumption. Molecule incubation parameters were optimized for the detection of low concentrations of fPSA. Spotting experiments demonstrated the possibility of sectioning a microfluidics device with different capture antibodies for various PCa biomarkers. This raises the possibility of measuring different analytes and cross-check results of the different molecules for a more accurate diagnosis. An aqueous two-phase system could be implemented for proteins extraction. In an attempt to decrease the assay time, molecules could be premixed with each other (e.g. capture antibody mixed with BSA) in order to decrease incubation time. The

measurements using photodiodes show the sensitivity of this biosensor to the enzymatic assay. The integration of PD detection eliminates the need for peripheral equipment, such as the microscope, allowing for the design of a miniature PoC device. All the detection methods were successfully integrated with the assay. To measure the fluorescence assay on the PD, a special filter (to cut the excitation light) needs to be deposited over the PD. This filter adds an extra number of steps to the microfabrication process of the PD. Chemiluminescence presents a further advantage for the PoC device development because it does not require a light source to be integrated into the system. A microfluidic capillary system can be implemented, eliminating the need for external pumps.

Bibliography

[1] September 2014. URL http://pubs.rsc.org/en/Content/ArticleLanding/2012/LC/c2lc20893h.

[2] September 2014. URL http://www.lasx.com/gallery/medical-applications/micromed-solutions/ativa-micro_web/.

[3] D. Huckle. Point-of-care diagnostics: an advancing sector with nontechnical issues. *Expert Rev Mol Diagn*, 8:679–688, 2008.

[4] Desmulliez M.P.Y Mohammed, M. Lab-on-a-chip based immunosensor principles and technologies for the detection of cardiac biomarkers: a review. *Lab Chip*, 11: 569–595, 2011.

[5] Kadimisetty K. Faria R. Rusling J.F. Sardesai, N.P. A microfluidic electrochemiluminescent device for detecting cancer biomarker proteins. *Anal Bioanal Chem*, 406: 3831—3838, 2013.

[6] Goryll M Sin L.Y.M. Wong P.K. Chae J. Choi, S. Microfluidic-based biosensors toward point-of-care detection of nucleic acids and proteins. *Microfluid Nanofluid*, 10:231—247, 2011.

[7] R. Mariella Jr. Sample preparation: the weak link in microfluidics-based biodetection. *Biomed Microdevices*, 10:777—784, 2008.

[8] Sullivan B.D. Mifflin R.L. Esener S.C. Heller M.J. Krishnan, R. Alternating current electrokinetic separation and detection of dna nanoparticles in high-conductance solutions. *Electrophoresis*, 29:1765—1774, 2008.

[9] Wilson J.A. Oakes S.G. Chiu S. Williams J.C. Pearce, T.M. Integrated microelectrode array and microfluidics for temperature clamp of sensory neurons in culture. *Lab Chip*, 5:97—101, 2005.

[10] Chamberlain M.D. Barbulovic-Nad I. Wheeler A.R. Bogojevic, D. A digital microfluidic method for multiplexed cell-based apoptosis assays. *Lab Chip*, 12:627––634, 2012.

[11] Haeberle S. Roth G. von Stettenz F. Zengerle R. Mark, D. Microfluidic lab on chip platforms: requirements, characteristics and applications. *Chem. Soc. Rev.*, 39:1153—1182, 2010.

[12] H. Kalish. Application of micro-fluidic devices for biomarker analysis in human biological fluids, biomedical engineering. *Research and Technologies*, pages 122––135, 2011.

[13] Linder V. Sia S.K. Chin, C.D. Commercialization of microfluidic point-of-care diagnostic devices. *Lab Chip*, 2012.

[14] R. Devarajan. Emerging urinary biomarkers in the diagnosis of acute kidney injury. *Expert Opin Med Diagn.*, 2:387—398, 2008.

[15] Nam Huh Suhyeon Kim Jeong-Woo Choib Jeong-Gun Lee, Kwang Ho Cheong and Christopher Koa. Microchip-based one step dna extraction and real-time pcr in one chamber for rapid pathogen identification. *Lab Chip*, 6:886—895, 2006.

[16] Prazeres D.M.F. Chu V. Conde J.P. Novo, P. Microspot-based elisa in microfluidics: chemiluminescence and colorimetry detection using integrated thin-film hydrogenated amorphous silicon photodiodes. *Lab Chip*, 10:777—784, 2011.

[17] González-Guerrero A.B. Dante S. Osmond J. Monge R.-Fernández L.J. Zinoviev K.E. Domínguez C. Lechuga L. M. Duval, D. Nanophotonic lab-on-a-chip platforms including novel bimodal interferometers, microfluidics and grating couplers. *Lab Chip*, 12:1987—1994, 2012.

[18] Didar-T.F. Veres T. Tabrizian M. Foudeh, A.M. Microfluidic designs and techniques using lab-on-a-chip devices for pathogendetection for point-of-care diagnostics. *Lab Chip*, 12:3249—3266, 2012.

[19] V. Jarrige. The need for a lower total psa cut-off value with psa assays calibrated to the new who standard. 2007.

[20] Radcliffe-C.M. Barrabés S. Ramírez M. Aleixandre R.N. Hoesel-W. Dwek R.A Rudd1 R.M. Peracaula R. de Llorens R. Tabarés, G. Different glycan structures in prostate-specific antigen from prostate cancer sera in relation to seminal plasma psa. *Glycobiology*, 16:132—145, 2006.

[21] Catto-J.W.F. Ward, M.A. and F.C. Hamdy. Prostate-specificantigen: biology, biochemistry and available commercial assays. *Ann.Clin. Biochem.*, 38:633—651, 2001.

[22] D.J. Heston W.D.W. Keefe. D.S.O., Bacich. Comparativeanalysis of prostate-specificmembrane antigen (psma) versus a prostate-specific membrane antigen-like gene. *The Prostate*, 58:200–210, 2004.

[23] Mucci L.A. Wilson K.M. Kraft P. Penney K.L. Stampfer-M.J. Giovannucci E. Shui, I.M. Common genetic variation of the calcium sensing receptor and lethal prostate cancer risk. *Cancer Epidemiol Biomarkers Prev.*, 22:118—126, 2013.

[24] Gu Z. Watabe T. Thomas G. Szigeti K. Davis-E. Wahl M. Nisitani S. Yamashiro J. Le Beau M.M. Loda M. Witte O.N. Reiter, R.E. Prostate stem cell antigen: A cell surface marker overexpressedin prostate cancer. *Proc. Natl. Acad. Sci.*, 95: 1735—1740, 1998.

[25] Gu J. Yoshida T. Wu X. Saeki, N. Prostate stem cell antigen: A jekyll and hyde molecule? *Clin Cancer Res*, 16:3533–3538, 2010.

[26] Yao X.D. Cao, D.L. Advances in biomarkers for the early diagnosis of prostate cancer. *Chin J Cancer*, 29:229–233, 2010.

[27] Judy Gibbs. *Selecting the Detection System - Colorimetric, Fluorescent, Luminescent Methods ELISA Technical Bulletin.*

[28] Tao S. Bova G.S. Liu A.S. Chan D.W. Zhu-H. Zhang H. Li, Y. Detection and verification of glycosylation patterns of glycoproteins from clinical specimens using lectin microarrays and lectin-based immunosorbent assays. *Anal. Chem.*, 83:8509—8516, 2011.

[29] Mikolajczyk SD Partin AW. Rittenhouse HG1, Finlay JA. Human kallikrein 2 (hk2) and prostate-specific antigen (psa): two closely related, but distinct, kallikreins in the prostate. *Crit Rev Clin Lab Sci*, 35:275–368, 1998.

[30] Cooperberg M.R. Cary, K.C. Biomarkers in prostate cancer surveillance and screening: past, present, and future. *Ther Adv Urol*, 5:318—329, 2013.

[31] Dosev D. Davies A.E. Gee S.J. Kennedy I.M. Hammock-B.D. Nichkova, M. Quantum dots as reporters in multiplexed immunoassays for biomarkers of exposure to agrochemicals. *Anal Lett.*, 40:1423—1433, 2007.

[32] Gitlin I. Stroock A.D Whitesides G.M. Ng, J.M.K. Components for integrated poly(dimethylsiloxane) microfluidic systems. *Electrophoresis*, 23:3461—3473, 2002.

[33] Kwon K.W. Park M.C. Lee S.H. Kim S.M. Suh-K.Y. Kim, P. Soft lithography for microfluidics: a review. *Biochip Journal*, 2:1–11, 2008.

[34] Ho C. Wong, I. Surface molecular property modifications for poly(dimethylsiloxane) (pdms) based microfluidic devices. *Microfluid Nanofluidics*, 7:291—306, 2009.

[35] Terry Pry David A Armbruster. Limit of blank, limit of detection and limit of quantitation. *Clin Biochem Rev*, 29, 2008.